米日

U.S. - JAPAN COORDINATED PROGRAM
FOR
MASONRY BUILDING RESEARCH

REPORT NO. 5.3-1

PLANK DIAPHRAGMS IN MASONRY STRUCTURES

by

MAX. L. PORTER
AZIZ A. SABRI
ROGER Y. KHOURY

July 1992

supported by:

NATIONAL SCIENCE FOUNDATION

GRANT NO. CES-8517028
FORMERLY GRANT NO. ECE-8517028

College of Engineering
Iowa State University

Na

This report presents the results of a research project which was part of the U.S. Coordinated Program for Masonry Building Research. The program constitutes the United States part of the United States - Japan Coordinated Masonry Research Program conducted under the auspices of the Panel on Wind and Seismic Effects of the U.S.-Japan Natural Resources Development Program (UJNR).

This material is based on work supported by the National Science Foundation under the direction of Program Director, Dr. S.C. Liu.

Any opinions, findings, and conclusions or recommendations expressed in this publication are those of the authors and do not necessarily reflect the views of the National Science Foundation and/or the United States Government.

Report No. 5.3-1

PLANK DIAPHRAGMS IN MASONRY STRUCTURES

by

Aziz A. Sabri, P.E., Ph.D., Instructor & Graduate Research Assistant;
Department of Civil and Construction Engineering
Town Engineering Building
Iowa State University
Ames, IA 50011

Max L. Porter, P.E., Ph.D., Professor;
Department of Civil and Construction Engineering
Town Engineering Building
Iowa State University
Ames, IA 50011

Roger Y. Khoury
Graduate Research Assistant
Town Engineering Building
Iowa State University
Ames, IA 50011

Francisco S. Yeomans
Graduate Research Assistant
Town Engineering Building
Iowa State University
Ames, IA 50011

Submitted to:
National Science Foundation
Grant No. BCS-8722870

Revised August 1993

TABLE OF CONTENTS

LIST OF TABLES

LIST OF FIGURES

1. INTRODUCTION

1.1. General

Masonry is one of the oldest building materials known to mankind. Due to its economic advantages and flexibility of construction, the use of concrete masonry has increased substantially over the past decade, particularly in the construction of medium to high rise buildings. A good knowledge of the basic structural components is essential and fundamental if rational design and analysis procedures are to be achieved. The different levels of concrete masonry include: ingredients (masonry units, mortar, grout, reinforcement), "microelements" (prisms, joints, other assemblies), "macroelements" (walls, diaphragms, connections), and full-scale structures [1].

Analytical and experimental studies have been conducted on ingredients and microelements by Mayes and Clough [2] and Hegemier [3]. A limited number of investigations have focused on the macroelement level. These studies include the compression, shear, and in-plane flexural behavior of walls [3,4], the biaxial response of walls [5,6], and the out-of-plane flexural response of walls and beams [7,8,9,10], and the behavior of the diaphragms [11].

Connections represent an important macroelement as they transmit direct and torsional shear, axial loads, and/or bending moments to floor diaphragms. The roof and floor diaphragms with the shear walls create a "box" shear-wall system that will not exist unless positive means are provided for transferring shear from the diaphragm into the shear walls. Lateral forces, typically produced by earthquakes or winds, are resisted by the use of a space frame system and/or shear walls. In either case, the lateral loads are transmitted from one wall to another through the floor system, as shown in Figure 1. For seismic design, one of the essential components in a structure is the slab or horizontal diaphragm.

The distribution of the horizontal forces to the shear wall or space frame system depends on the properties of the diaphragm slab, the connecting elements, and the resisting system (i.e. shear wall or space frame). In the case of a shear wall building, the diaphragm can be considered to be a horizontal beam with the roof or the floor acting as the web of the beam. With simple, transverse lateral loads, the forces flow out to the shear walls as is shown in the force distribution diagram given in Figure 2. In order to optimize the performance of the floor system, the in-plane stiffness of the diaphragm should exceed that of their respective vertical subsystems. Diaphragms of this type are categorized as rigid [12, 13] (refer to Figure 3 for a conceptual sketch). In such case, the diaphragms act as a flat plate that transmits lateral loads to the vertical bracing elements in proportion to their relative rigidities. Conversely, with flexible diaphragms, loads are distributed to vertical subsystems as a continuous beam using tributary areas. Regardless, both rigid and flexible systems should be able to retain a sufficient amount of in-plane

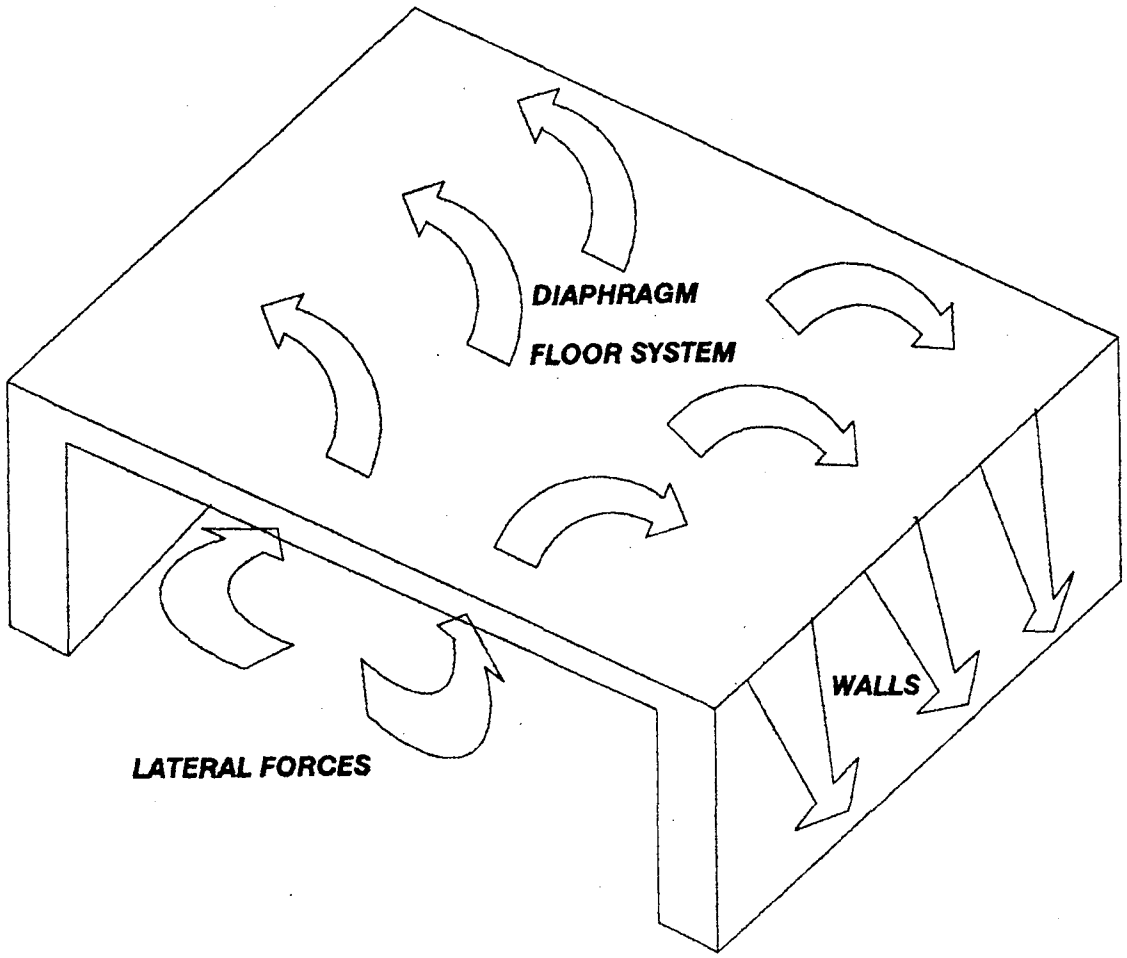

Figure 1. Lateral force distribution [11]

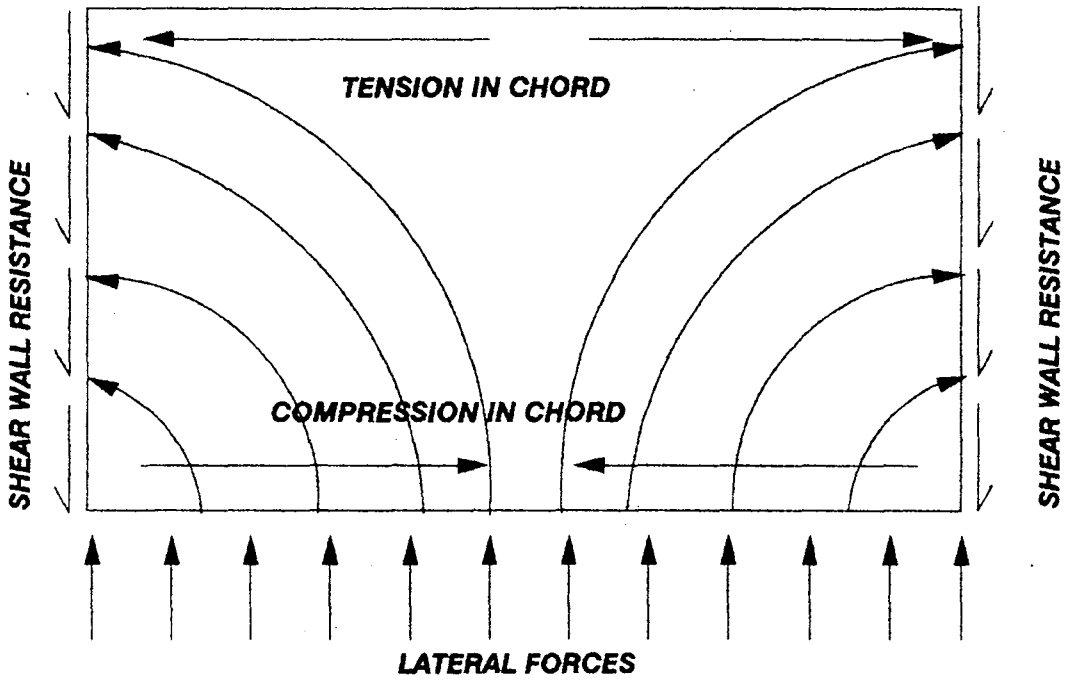

Figure 2. Schematic force distribution diagram [11]

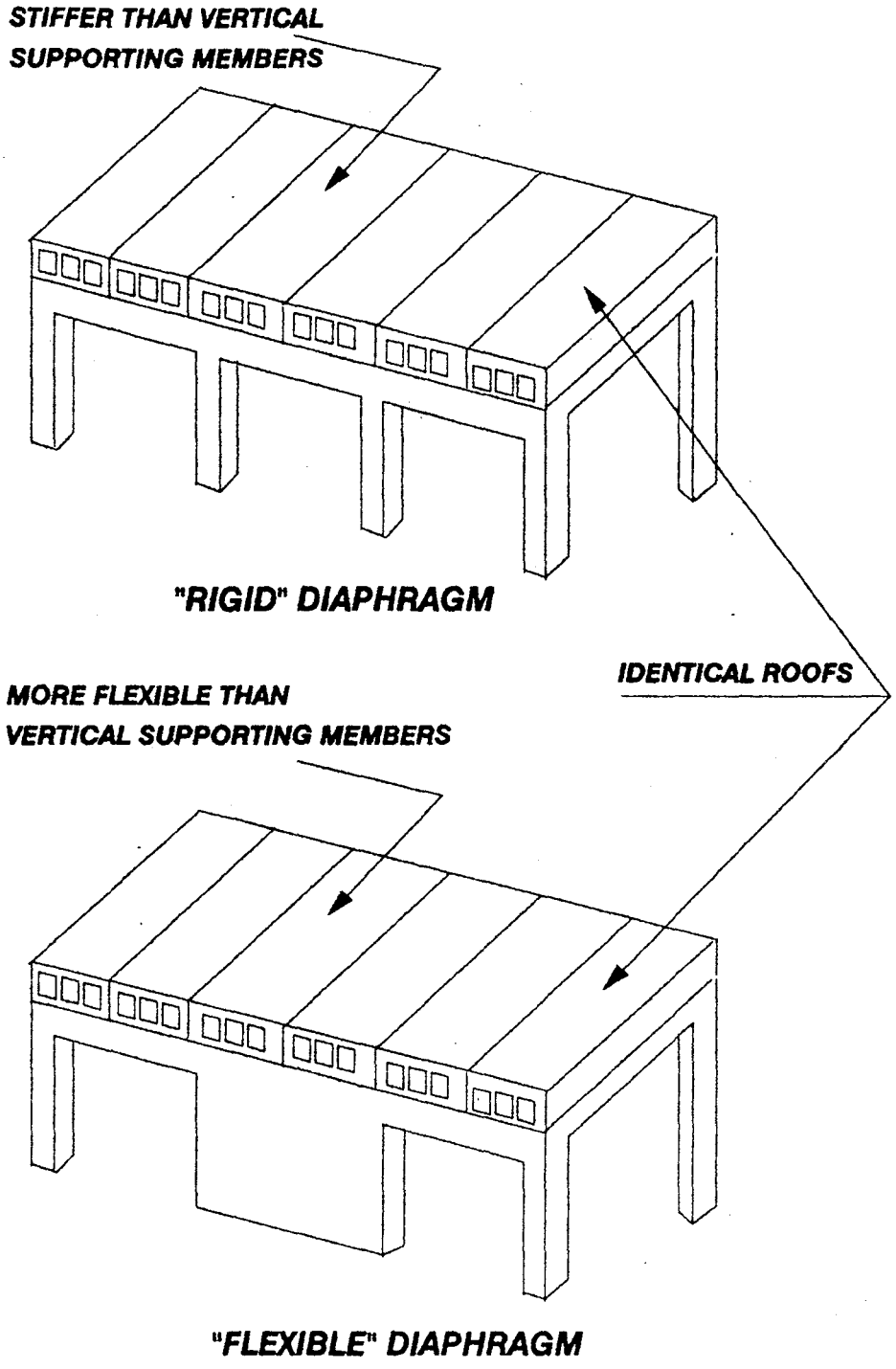

Figure 3. Diaphragm stiffness classification

stiffness or strength in order to prevent collapse, well beyond the elastic range. Hollow-core planks are used in masonry buildings as roof and floor diaphragms. A typical building floor construction utilizing precast, prestressed planks is shown in Figure 4. The behavior of hollow-core plank diaphragms under seismic loads has been investigated in Task 5.1 of The Technical Coordinating Committee of Masonry Research (TCCMAR). The results of this investigation were summarized in Reference 11.

1.2. Objective of the Overall Research Program

The research undertaken for this project is part of the U.S.-Japan Coordinated Program for Masonry Building Research. Each category of this program is conducted under the supervision of the Technical Coordinating Committee for Masonry Research (TCCMAR). The TCCMAR committee was organized to function under the auspices of the Panel of Wind and Seismic Effects of the U.S.-Japan Cooperative Program in Natural Resources (UJNR). Study of floor diaphragms, which is the objective of this project, is the fifth research task of the TCCMAR coordinated program. Additional information on the organization of the Masonry Building Research Program is available in Reference 14.

The objective of the overall TCCMAR research program is to elevate masonry structural analyses, design, and construction practice to a level comparable to structural steel and reinforced concrete technology [14].

1.3. Objective and Scope of Task 5.3

The TCCMAR research program on diaphragms was the subject of this work conducted at Iowa State University (ISU). The research project on concrete diaphragm characteristics was divided into three separate tasks. Task 5.1 involved the experimental and analytical investigation of precast horizontal diaphragms subjected to in-plane loading. Task 5.2 focused on the collection of existing literature and data generated from the discussion and testing of horizontal diaphragms. Task 5.3 included full-scale testing of a box wall-to-floor specimen and associated analytical studies. This report is devoted to the findings on Task 5.3. Separate reports have been issued for Tasks 5.1 and 5.2 [11, 15].

The objectives of this research project were to determine the basic failure modes, ascertain behavioral characteristics, and investigate analytical properties for the full-scale testing of precast, prestressed hollow-core plank diaphragms supported by masonry walls and subjected to in-plane shear. The main focus of this study is to replace the steel beams utilized in Task 5.1 with masonry walls and study the effects on the diaphragm behavioral characteristics. This testing arrangement is shown in Figure 5 and the previous task arrangement is shown in Figure 6. The basic characteristics include stiffness, First Major Event (FME) load, ultimate load, failure mode, and hysteretic behavior.

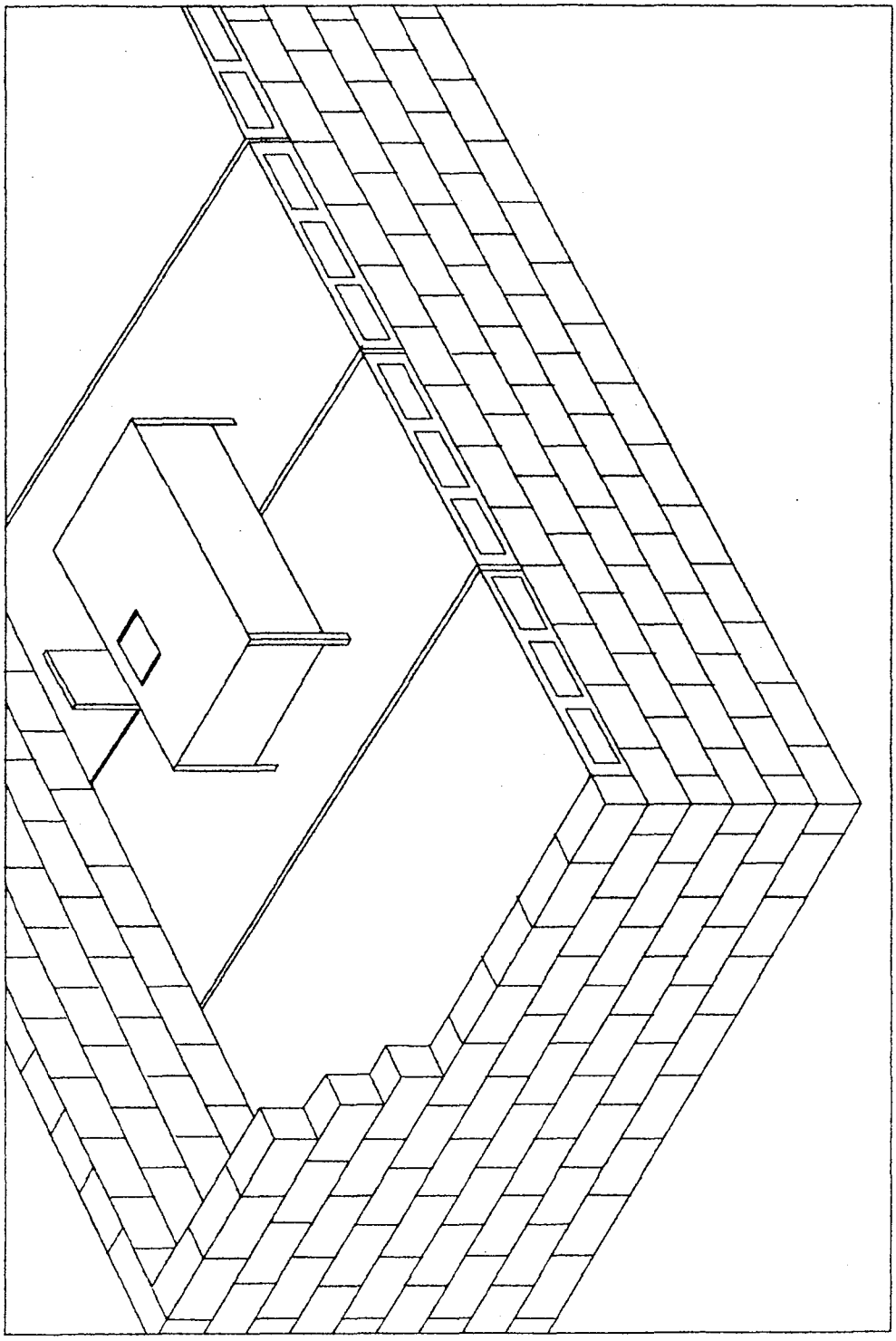

Figure 4. Typical building floor utilizing hollow-core planks

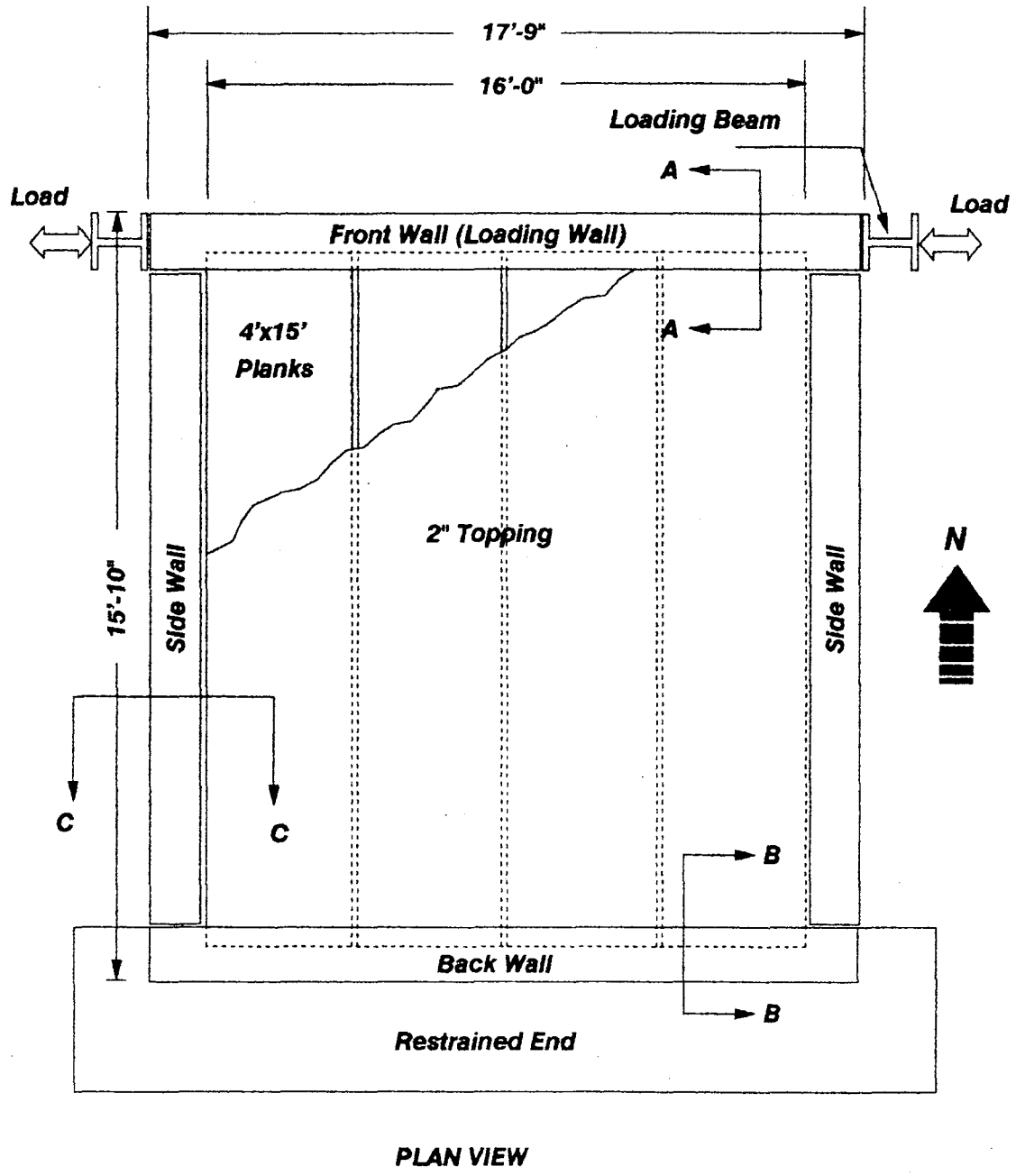

Figure 5. Schematic of testing frame for Task 5.3

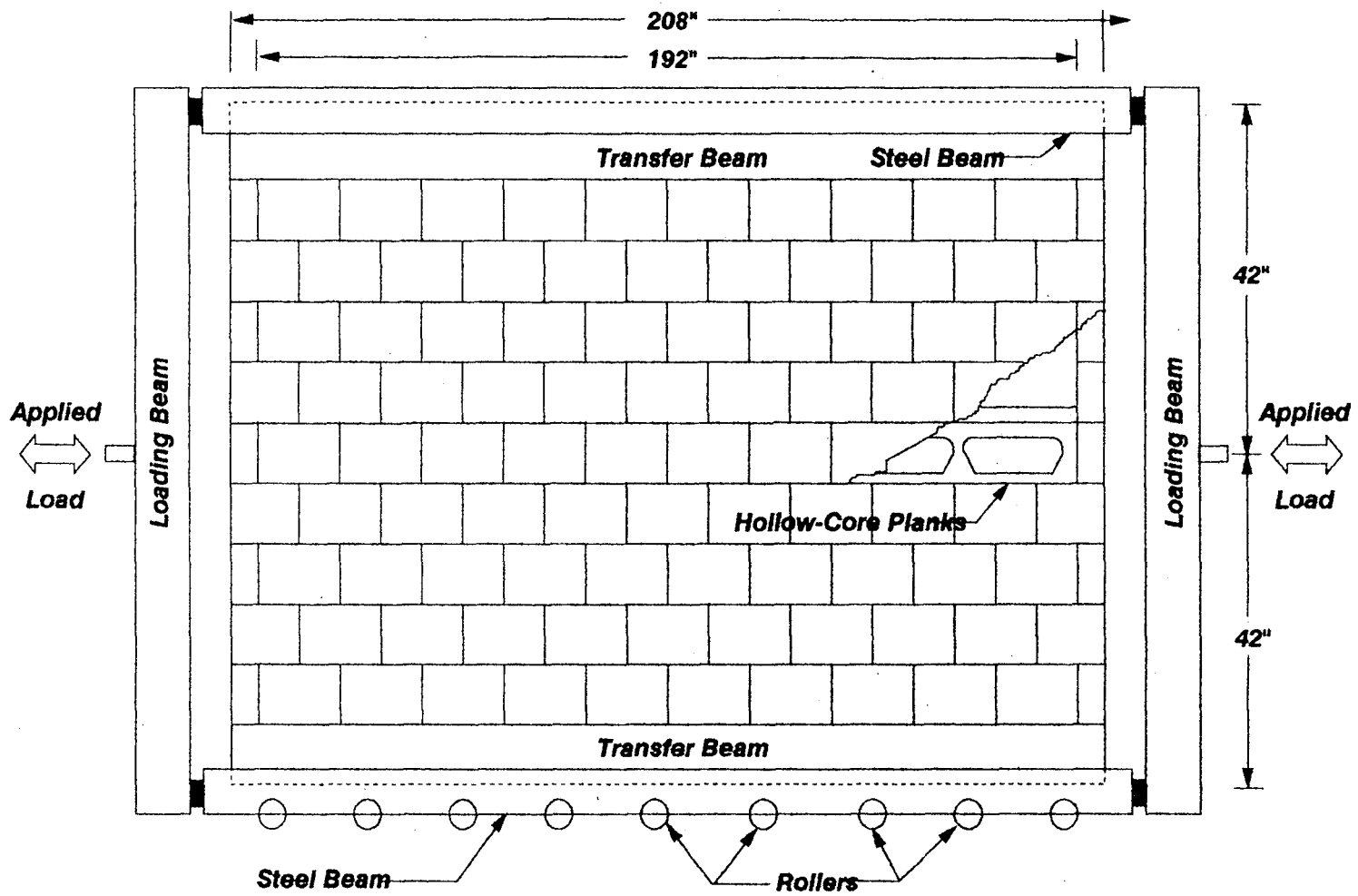

Figure 5. Continued

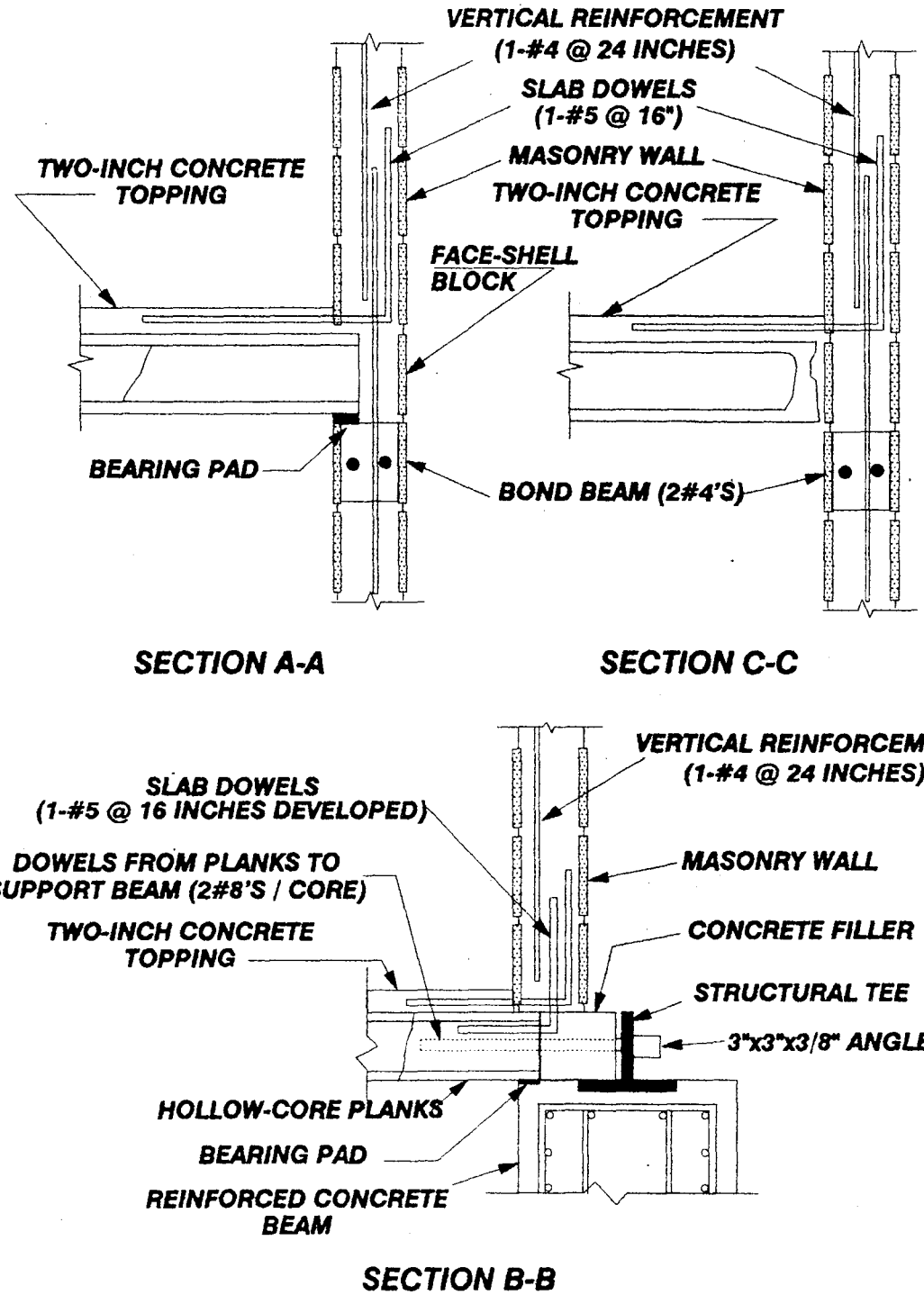

Figure 5. Continued

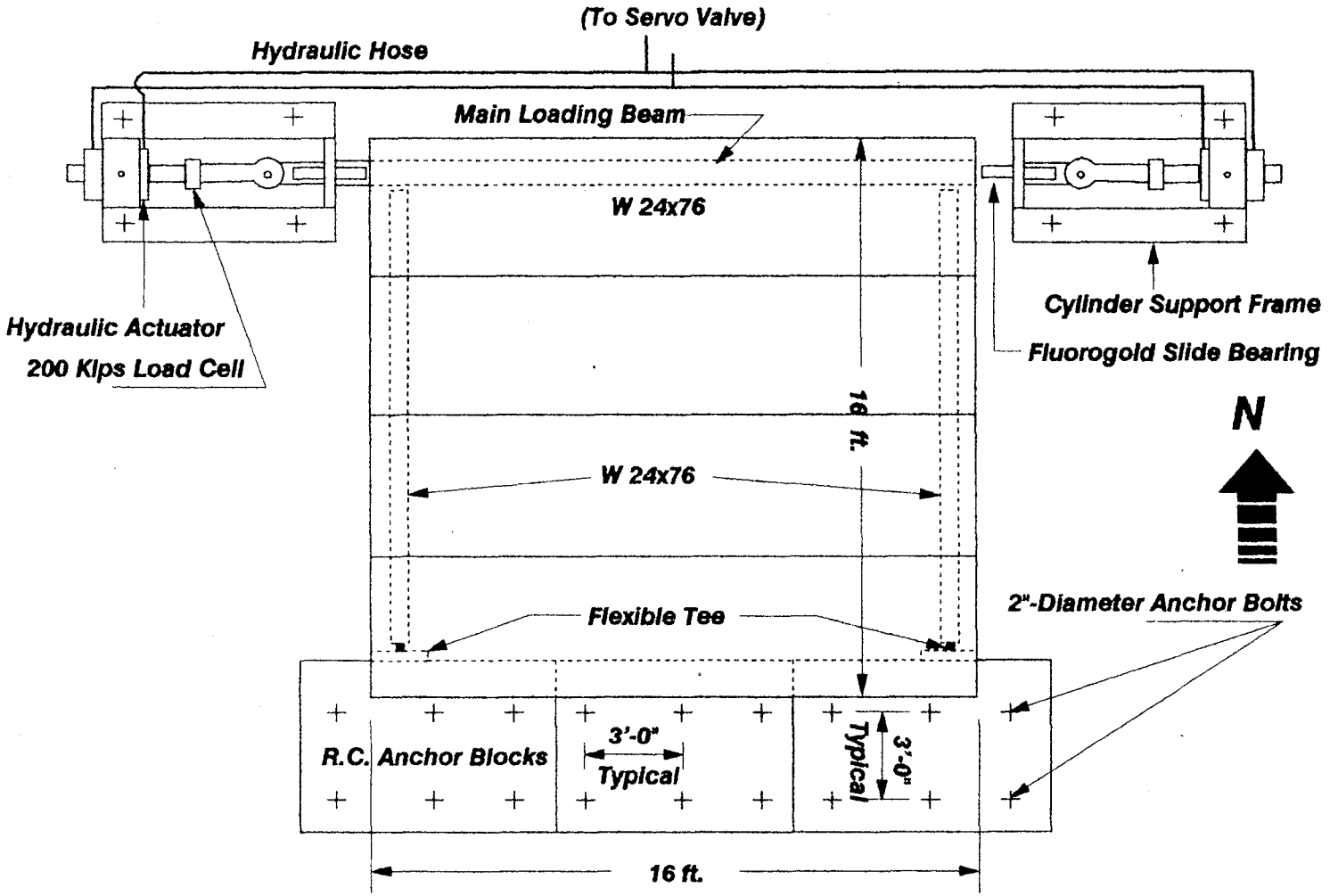

Figure 6. Schematic testing frame for Task 5.1 [11]

One connection type, was chosen based on its frequent recurrence in multistory concrete masonry field practice. Also the options of different connection details were narrowed down by selecting initial four connection details practically used in seismic zones. The selection was based on discussions with a number of prominent structural engineers who are experienced in the seismic design of masonry structures. The four initial connection details were subjected to further discussions and finally two were selected based on their practical application with plank diaphragms.

2. REVIEW OF RELATED RESEARCH

2.1. General

A well designed diaphragm is essential for the structural integrity of a building during earthquake or wind induced motions. Shear forces caused by lateral loads are distributed to the various elements of the structure in proportion to their rigidities relative to that of the diaphragm. Unless the structure has been properly designed to resist those forces, collapse or serious structural damage will occur.

These in-plane forces are distributed to the various essential elements of the lateral load resisting box system through an appropriate connection detail at the floor and roof diaphragm boundary. The importance of diaphragm action in a structure was demonstrated during the 1964 Anchorage, Alaska earthquake. Two structures, the Chrysler Center Auto Showroom and the partially completed Alaska Sales and Service Building, both collapsed due to inadequate integral behavior [16]. Thus, knowledge of the behavioral characteristics of such a system is necessary to provide lateral stability to the building.

There are four absolutely essential structural components which comprise this box system; namely: (1) those walls perpendicular to the direction of the lateral loads, (2) the horizontal roof and floor diaphragms, (3) the shear walls parallel to the lateral load direction, and (4) the connections of the walls to the floors. The following subsections review past research that relates to the behavioral and design characteristics of some of the essential components that comprise the system.

2.2. Precast Concrete Diaphragms

Diaphragms may be categorized according to their composition into the following common types: cold-formed steel, non-composite fills with various decking, composite steel deck, timber, reinforced concrete, and precast concrete. Each of these groups are similar in that they provide in-plane shear resistance, but they exhibit unique behavioral characteristics. During previous seismic events, the performance of precast concrete units without topping has been poor, while the precast concrete units with topping have

exhibited variable to good performance [17]. Most of the past work pertaining to precast concrete diaphragm focused on untopped units. Furthermore, the majority of the previous research concentrated on the behavior of joints between precast elements. Grouted joints between adjacent planks have been tested under direct shear. Martin and Korkosz [18] stated that the absence of continuity and redundancy between the precast slabs has caused some designers to question the stability of precast structures under high lateral loads. The Prestressed Engineering Association of Japan points out that a prestressed concrete system may absorb less energy than that assumed in the typical elasto-plastic earthquake response because of deficient hysteresis properties [19].

The stiffness and strength of precast units interconnected to achieve diaphragm action is a major consideration. Mechanical ties between units in grouted keyways are generally used along with a properly reinforced cast-in-place topping. Structural integrity must be maintained by adequate horizontal, vertical, and peripheral ties between all structural units. When planks are oriented in the direction perpendicular to the lateral force direction, the ties (peripheral) are necessary across the ends of the units to clamp them together while similar ties act as tensile units minimizing out-of-plane deformations when planks are laid parallel to the load direction [20].

Tanner Prestressed and Architectural Company [21] conducted some tests to investigate the shear strength of the grouted horizontal shear joint in planks. Each of their specimens consisted of three sections joined together and loaded in the center in order to transfer the load equally through the seams. Test results showed longitudinal shear crack propagating along the grout plank interface.

An experimental investigation of the shear diaphragm capacity was undertaken by Concrete Technology Associates in 1972 [17]. This investigation focused on the horizontal shear transfer strength through grouted longitudinal joints without shear keys as well as determining the friction coefficient. Three sections were tested by fixing the outer slabs and applying the load to the center unit. Since the shear friction coefficient was one of the test objectives, the shear strength was not carried to ultimate capacity. The coefficient of friction was found to vary between 1.30 and 2.00.

Another experimental study was conducted by Reinhardt and Hartjes [22] to investigate the shear strength of horizontal joints between planks. Parameters considered were the mortar strength and the joint length. The length of the joint was found to have a significant effect on the shear stress at fracture. The failure mode of each of the tests was brittle fracture of the bond at the mortar and grout interface.

2.3. Connections

The first major experimental work on connections was reported by Sahlin [23] in 1969. This study contains some full-scale brick exterior walls and concrete floor slabs:

(1) floor slab extending completely through walls, (2) floor slab partially extending through walls, and (3) roof connections. These tests were intended to establish a relationship between the static moment and the angle of rotation in the joints.

In 1978 Harris and Becica [24] reported an investigation of the failure and response characteristics of 1/4 scale concrete masonry interior wall to hollow-core precast concrete slab connections subjected to axially applied gravity-type loads. Included in this test series were four specimens with horizontal joints, reinforced and unreinforced.

In 1978 Gülkan, et al. [25] reported experiments on 19 full-scale timber roof connection models subjected to cyclic in-plane and/or out-of-plane forces. Walls were partially grouted masonry bearing and non-bearing walls with both gable and flat room construction. These specimens represent the connections of typical one story residential or industrial buildings.

In 1982 Anvar [1] conducted a study on the behavior of connections in concrete masonry buildings at the University of California, San Diego, California. The primary objective of the experimental portion of this program was to obtain basic information on strength, stiffness, and damping characteristics of such connections subjected to monotonic and cyclic shear loading. Three major types of connection were selected for testing: (1) precast, reinforced concrete slabs supported by an interior concrete masonry wall, (2) cast-in-place slab supported by interior wall, and (3) hollow-core, prestressed concrete plank with or without topping supported by an interior wall. All walls were reinforced and fully grouted. The overall size of the specimen was 64 inches-wide, 64 inches-high, and 8 inches-thick concrete blocks (nominal).

In 1978 Hawkins [19], reviewed the results of analytical and experimental studies concerning the seismic resistance of prestressed and precast concrete structures and their subassemblages. He stated that the weak point in precast construction is the joints. While it is desirable that connections be ductile and stronger than the units joined, such conditions are extremely difficult to satisfy. Unless cast-in-place connections, grouting or post-tensioning are used, connecting elements must themselves be anchored in the precast panels and then those anchors become the weak elements.

2.4. Mechanisms of Shear Transfer Across Concrete Interfaces

Experimental and analytical studies have been conducted to study the shear strength of connections. Concrete masonry connections are similar in nature to precast and cast-in-place joints in slabs and shear walls. From previous studies, three mechanisms of shear transfer across concrete interfaces have been identified [26,27,28] to contribute to the shear strength of connection, namely: bond, interface shear transfer and dowel action. The conclusion that can be drawn from these investigations is that the shear strength of a connection is largely affected by the interface shear transfer phenomenon [28]. The

basic phenomenon of interface shear transfer is the aggregate interlocking contribution generating frictional and bearing forces between the two faces of the joint or crack when subjected to shear loading [28,29,30].

Birkeland and Birkeland [31] and Mast [32] showed that the frictional forces can contribute to the shear transfer mechanism of a joint if normal restraint is provided. The restraint can be achieved by the transverse reinforcement across the joint or crack.

Loeber and Paulay [33] investigated the interface shear transfer mechanism by performing direct shear tests on pre-cracked concrete blocks. The purpose of this investigation was to evaluate the effect of the crack width and aggregate shape and size on the shear strength under monotonic and cyclic loading. The results indicated that the stiffness of the interface shear mechanism is not significantly influenced by the shape and size of aggregates. The conclusion that can be drawn from this and other investigations is that cycling the load decreases the interface shear transfer stiffness and increases the interface separation.

In the experimental domain, a substantial number of investigations have reported the dowel effect on transferring shear forces across joints. This was first observed in studies on contraction joints in pavement slabs and/or shear strength of reinforced concrete beams. The previous studies indicated that the dowel stiffness decreases with the deterioration of the surrounding concrete [29,34,35]. This deterioration is a function of the tensile strength of the concrete, the axial stress in the dowel, the size and cover of reinforcement and the externally applied precompression stresses.

In addition, some researchers have also studied the effect of interface shear transfer combined with dowel action [26,29,31,35]. The studies concluded that the interface shear transfer mechanism carried between 65 and 75% of the total shear load while the remaining 35 to 25% was resisted by the dowel action mechanism [29,35].

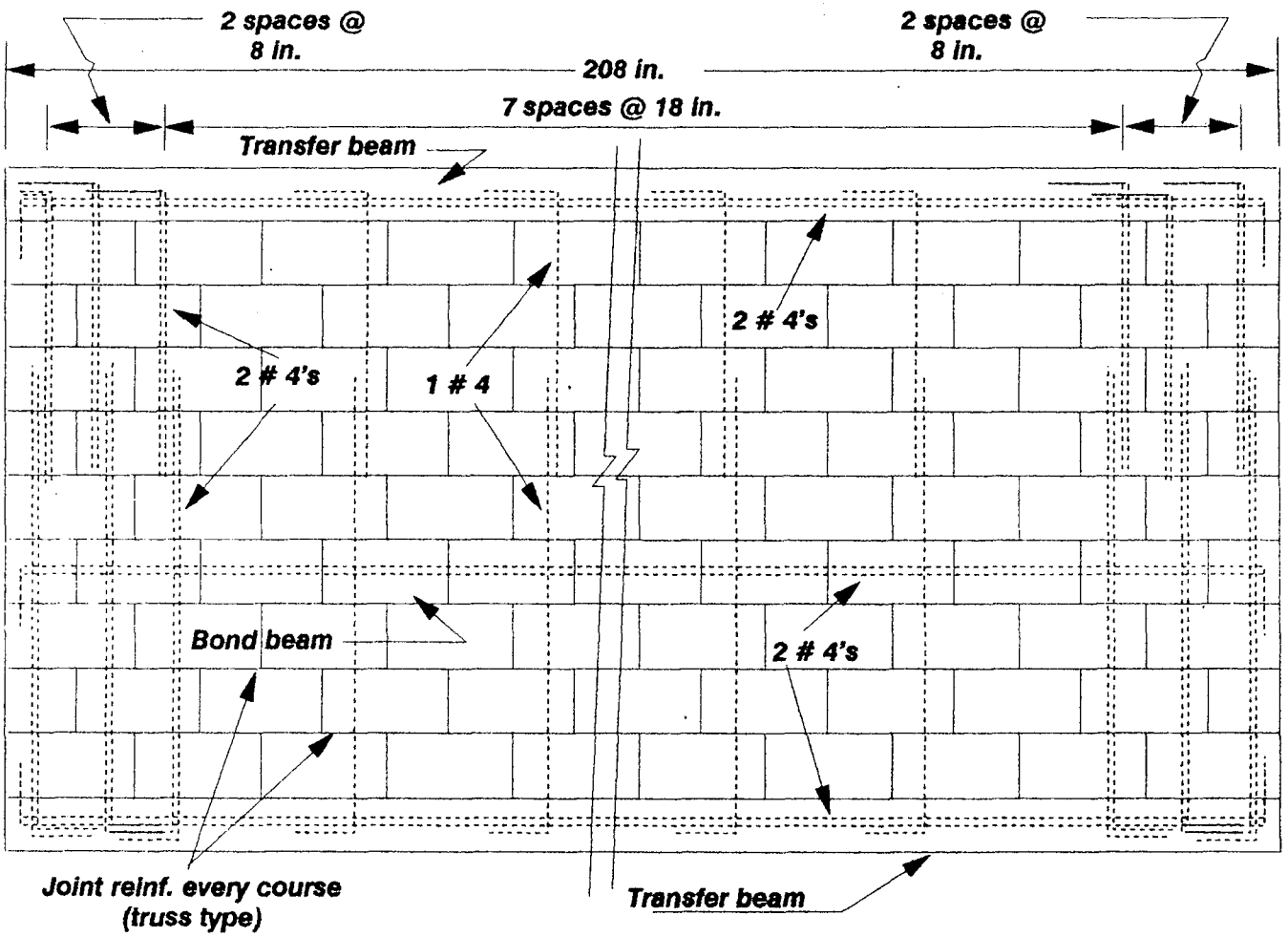

Figure 7. Reinforcement distribution in the walls

3. EXPERIMENTAL PROGRAM

3.1. General

The experimental program was designed to provide additional data on precast, prestressed hollow-core plank diaphragms in concrete masonry structures subjected to in-plane loading. The main objective of this portion of the program focuses on the effect of the supporting masonry wall on the behavioral and strength characteristics of the floor diaphragm. The wall details were chosen to produce the initial failure in the diaphragm or connections.

3.2. Test Specimen

Elevation and plan views with dimensions of the specimen are shown in Figure 5. The specimen height represented approximately half-story height above and below the slab diaphragm. The overall dimensions of the specimen were 15 ft. by 16 ft. for the diaphragm and 7 ft. high for the walls. The following subsections discuss the different components in more detail.

3.2.1. Walls

The masonry wall elements were designed to withstand the predicted failure load of the system. This was based on the previous diaphragm tests in Task 5.1. The ultimate load of similar plank diaphragm was attained at approximately 300 kips [11]. Each wall consisted of two-cell hollow standard concrete block (regular stretcher), single corner (one plain end), solid slab (1 1/2 thick nominal), and bond beam blocks laid in running bond with 3/8 in. thick mortar bedding. Bed joints consisted of full mortar coverage on the face shell and the webs. Mortar was also applied at the face-shell ends of blocks for head joints.

All walls were reinforced both vertically and horizontally and fully grouted. The walls were approximately 17.33 ft. long and 7 ft. high for the front wall while the side walls were approximately 15.83 ft. long and 7 ft. high. The walls were constructed with a single wythe of 8 x 8 x 16 in. hollow concrete block, and consisted of four courses above and below the slab in addition to reinforced concrete top and bottom beams. The walls were uniformly reinforced with additional reinforcement near the ends to resist the induced moment resulting from applying the load at the top and bottom of the walls. A total of 18 No. 4 bars were placed in each wall as the vertical reinforcement (see Figure 7 for bar distribution), and truss type joint reinforcement was used in every joint as the horizontal reinforcement. In addition, 2 No. 4 bars were placed horizontally within the bond beam under the floor level and all around its perimeter.

3.2.2. Floor

The floor diaphragm consisted of four prestressed, precast hollow-core planks. The planks were 4 ft. wide, 15 ft. long, and 8 in. thick. Figure 8 shows a typical cross section of an eight-inch thick plank. The planks were constructed of normal weight, high-strength concrete. A two-inch concrete topping was placed on top of the planks after the walls were constructed and grouted. The cores of the planks were filled with grout for approximately 18 in. from the edge. Styrofoam inserts were placed in the cores, to prevent the grout from flowing too far inside the cores.

3.2.3. Connections

The selection of the connection type and details was based on typical connections encountered in medium to high rise reinforced concrete masonry buildings. This was accomplished based on discussions with a number of prominent structural engineers and members of the TCCMAR group who are experienced in the seismic design of masonry structures. The connections details are shown in Figure 5.

3.3. Materials and Material Properties

All test specimen components were built from commercially available materials, typical of those commonly used in masonry building construction.

3.3.1. Concrete block units

The units used in the construction of this specimen were nominally 8 x 8 x 16 in. standard two-cell hollow blocks (stretcher), 8 x 8 x 16 in. corner blocks, 1 1/2 x 8 x 16 in. solid slabs, and 8 x 8 x 16 in. 2 1/2 in. cut bond beam blocks. These units are shown schematically in Figure 9. Four of each unit type (except bond beam units) were measured and tested, according to ASTM C140-86 [36] standards. The dimensions and material properties of units are listed in Tables 1 and 2, respectively. The results of the average compressive strength of the units are summarized in Table 3.

3.3.2. Mortar

Type "S" mortar mixed with volume proportions of 1:1/2:3 1/2 (cement: lime: sand). The mortar was mixed in an electric mixer to a workable consistency with water added as necessary. Nine 2 x 4 in. cylindrical mortar samples (UBC Standard No. 24-22) [37] were taken during the construction at different stages. All mortar specimens were cured similar to the test walls, capped with sulfur and tested according to ASTM C270-86 standards [36]. Table 4 shows a summary of the results of the compressive strength for these mortar specimens.

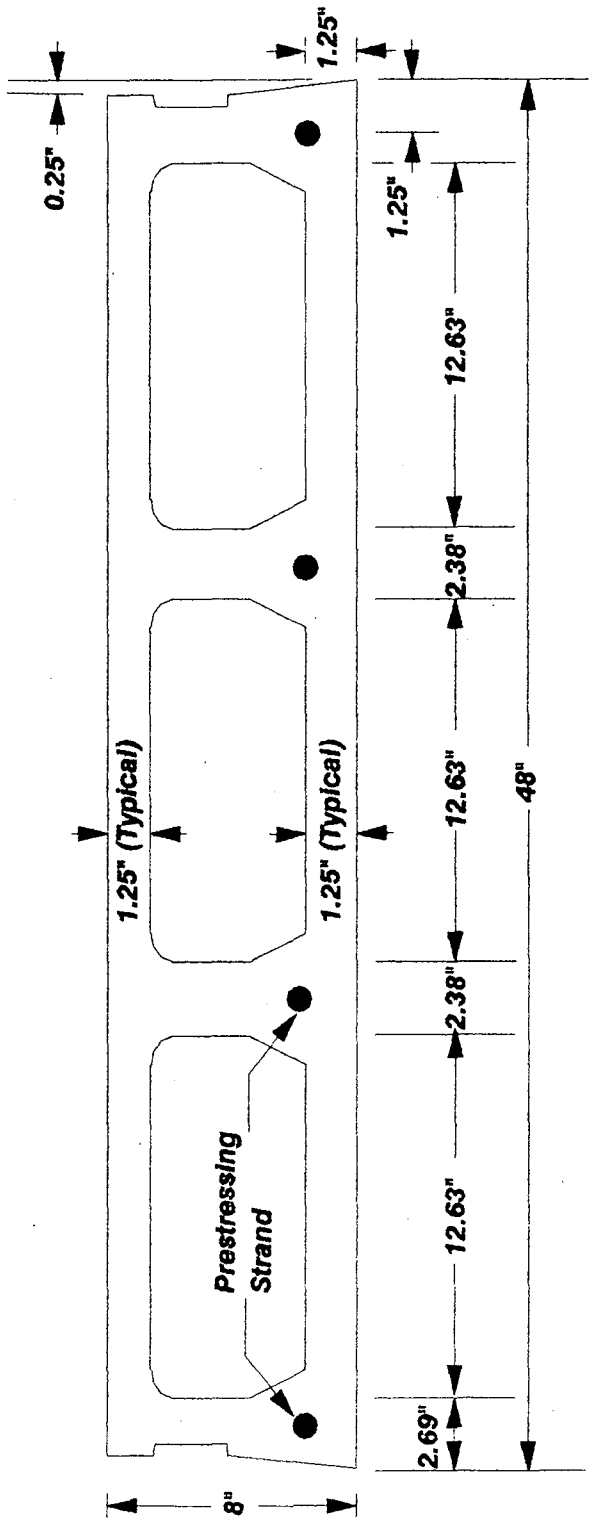

Figure 8. Typical cross section of eight-inch planks

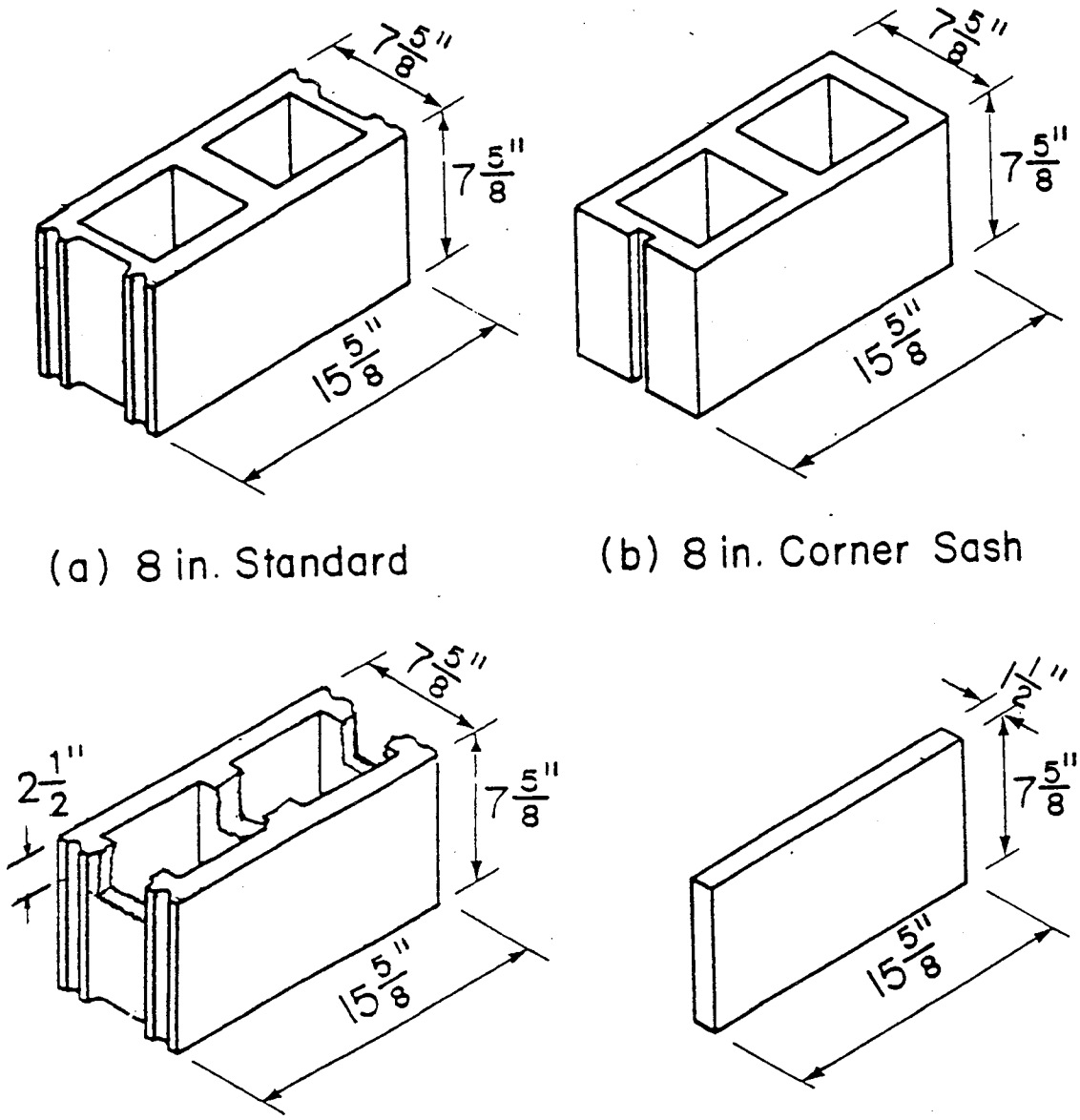

Figure 9. Masonry units

Table 1. Dimensions of concrete masonry units

Block Type	No. of Units Measured	Length (in.)	Width (in.)	Height (in.)	Face-Shell Thickness, min. (in.)	Web Thickness, min. (in.)	Gross Area ($in.^2$)	Avg. Area ($in.^2$)	Net % of Gross
8"x8"x16" Standard	4	15.623	7.610	7.325	1.25	1.00	118.89	63.61	53.50
8"x8"x16" End corner	4	15.550	7.633	7.610	1.25	1.00	118.69	62.50	52.66
1 1/2"x8"x16"	4	15.520	1.523	7.625	-	-	23.64	23.64	100.

Table 2. Material properties of concrete masonry units

Block Type	No. of Units	Absorption (lb/ft^3)	Absorption %	Moisture Content
8"x8"x16" Standard	4	10.40	6.88	12.31
8"x8"x16" End Corner	4	14.43	18.03	6.50
1 1/2"x8"x16" Solid Slab	4	8.30	5.62	15.42

Table 3. Summary of compressive strength of concrete masonry units

Block Type	No. of Units tested	Ultimate Load (kips)	Compressive Strength (psi)	
			Gross Area	Avg. Net Area
8"x8"x16" Standard	4	222.4	1867	3496
8"x8"x16" End Corner	4	157.0	1318	2512
1 1/2"x8"x16" Solid Slab	4	100.2	4282	4282

Table 4. Summary of compressive tests on grout, mortar, and concrete-topping samples

Strength Material	Specimen Type	Average Compressive Strength (psi)
Grout	3"x3"x6" Block-Molded	4050
	3"x6" Cylinder	2560
	2"x4" Cylinder	2401
Mortar	2"x4" Cylinder	2880
Concrete Topping	6"x12" Cylinder	7233
	3"x6" Cylinder	5994

3.3.3. Grout

The grout was mixed with volume proportions of 1:3:2 (cement: sand: pea gravel) with a slump of 8-10 in. (ASTM C476-86) [36]. The grout mix was delivered to the laboratory by a local ready-mixed and concrete manufacturer. In addition, an admixture: SIKA Grout Aid, Type II, was added to the grout as a plasticizing agent at the construction site with a proportion of 1 lb. to every 94 lbs. of Type II Portland cement. Grout specimens were obtained in three forms: 3 in. diameter by 6 in. high, 2 in. diameter by 4 in. high non-absorbent cylinders, and 3 in. square by 6 in. high block molded specimens conforming to ASTM E447 [36]. Twenty-seven samples were made altogether, nine of each, and cured alongside the specimen at the same atmospheric conditions. All samples were capped with sulfur mortar and tested in accordance with ASTM E447 [36]. The results from the grout tests are shown in Table 4. The non-absorbent cylinders yielded a lower grout strength due to the high water/cement ratio of the grout mix, whereas the molded specimens resulted in higher strength due to the initial absorption by the molds.

3.3.4. Concrete

The two-inch concrete topping was cast after the top walls had been built. The concrete was delivered by a local ready-mix concrete manufacturer with a specified minimum 28-day strength of 5 ksi and a specified slump of 3 in. A total of fifteen concrete test cylinders, nine 6 in. diameter by 12 in. high and six 3 in. diameter by 6 in. high, were cast and tested in accordance with ASTM E447 Standards [36]. A summary of the results of the concrete tests is given in Table 4.

3.3.5. Reinforcing steel

All reinforcing bars used were deformed Grade 60 steel. No. 4 bars were used as vertical reinforcement in the walls and horizontal reinforcement in the bond beam. No. 9 gage diagonal truss joint reinforcement was used as horizontal reinforcement. No. 5 bars were used as slab dowels for the connection. Table 5 shows the average properties of the reinforcing bars.

3.3.6. Prisms

Twelve single block prisms were constructed and tested. All the prisms were two blocks high, as shown in Figure 10. They were built at the time the full-scale specimen was constructed using the same techniques and workmanship as the walls. All prisms had full mortar bedding with tooled joints. Eight fully grouted and four ungrouted prisms were built, cured, capped, and tested in accordance with ASTM E447-86 Standards [36]. The grouted prisms were cut along the face of the central web due to the high load required to fail the complete prisms. Figure 10 shows the original and cut prisms.

Table 5. Physical properties of reinforcing steel

Bar	Yield Stress δ_y, (ksi)	Yield Strain ϵ_y, (in/in)	Ultimate Stress δ_{ult}, (ksi)	Modulus of Elasticity E_s, (ksi)
#4	58.8	0.00199	79.1	29.5×10^3
#5	63.2	0.00205	80.3	30.8×10^3
Truss Type Joint Reinf.	Not verified			

3.4. Construction of Full-Scale Specimen

The construction of the full-scale test specimen took place as explained in the following sections:

3.4.1. Building the base transfer beams

Two groups of beams were built to transfer the load from the loading beam to the masonry wall. The bottom beams were cast in channel sections with shear studs. The steel beams were supported on steel rollers to reduce friction. Dowels for the wall reinforcing (with 90-degree hooks) were embedded in the concrete.

3.4.2. Construction of the bottom wall

Four courses of masonry blocks were constructed on top of the bottom transfer beams. Three of these courses utilized standard hollow masonry blocks. The last course consisted of transfer beam units to allow for the placement of horizontal reinforcing bars (two No. 4) underneath the planks.

3.4.3. Placement of the hollow-core planks

Four hollow-core planks were placed on top of the bottom wall. The planks were oriented in the north-south direction perpendicular to the load. Solid masonry face-shell blocks were placed in the front wall at the plank level (see Section A-A in Figure 5). This allowed the diaphragm to partially rest on the wall (front only). The other end of the

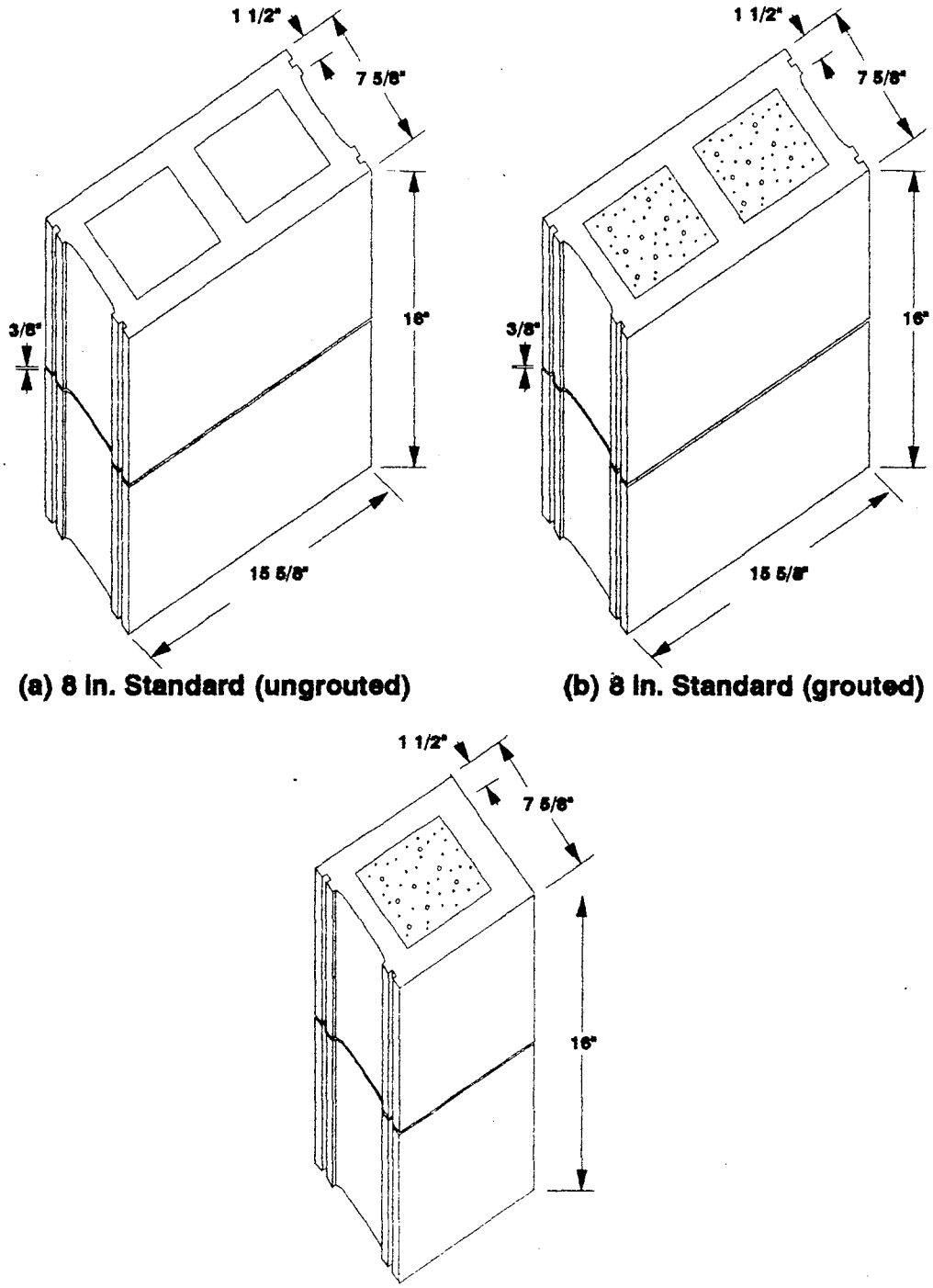

Figure 10. Masonry prisms

planks was connected to a rigid concrete beam and supported by the concrete blocks (refer to Section B-B of Figure 5) at the restrained end. Reinforcing dowels (No. 5 @ 16") were then placed in the topping to connect the planks to the walls all around the perimeter.

3.4.4. Construction of upper walls

Four more courses of masonry blocks were placed above the plank level. The dowels from the plank topping were placed inside the blocks (see Figure 5).

3.4.5. Placement of concrete topping

A two-inch concrete topping was poured on top of the planks. The reinforcing dowels were raised slightly to allow for the concrete cover.

3.4.6. Grouting of the walls

The walls were grouted solid with mortar. The vertical reinforcement of the upper walls extended about 4 inches above the last course. This reinforcement was anchored in the top bond beam.

3.4.7. Casting of the top transfer beam

The final step was the casting of the top transfer beam. This beam served to transfer the load from the loading beam to the walls, as discussed earlier.

3.5. Test Set-Up

3.5.1. Test facility

A horizontal cantilever test frame was designed for this project. Figure 11 shows a schematic plan view of the testing frame. The restrained edge was used to model continuous attachment of the specimen to a shear wall or an adjacent slab and was formed by large reinforced concrete blocks anchored to the test floor with 2 in. diameter high strength bolts. The free edges were the masonry walls that were constructed on steel beams supported by rollers. A structural steel tee was embedded into the reaction concrete block to attach the specimen to the restrained edge (see Section B-B, Figure 5).

Two H-shaped steel beams, with plates welded to the flanges, were used as vertical members to transfer the applied horizontal load to the front wall. Front view of the specimen and loading frame is schematically shown in Figure 12. The vertical steel members were connected to the horizontal steel members, located at the top and the bottom of the specimen's front wall, by flexible tee joints.

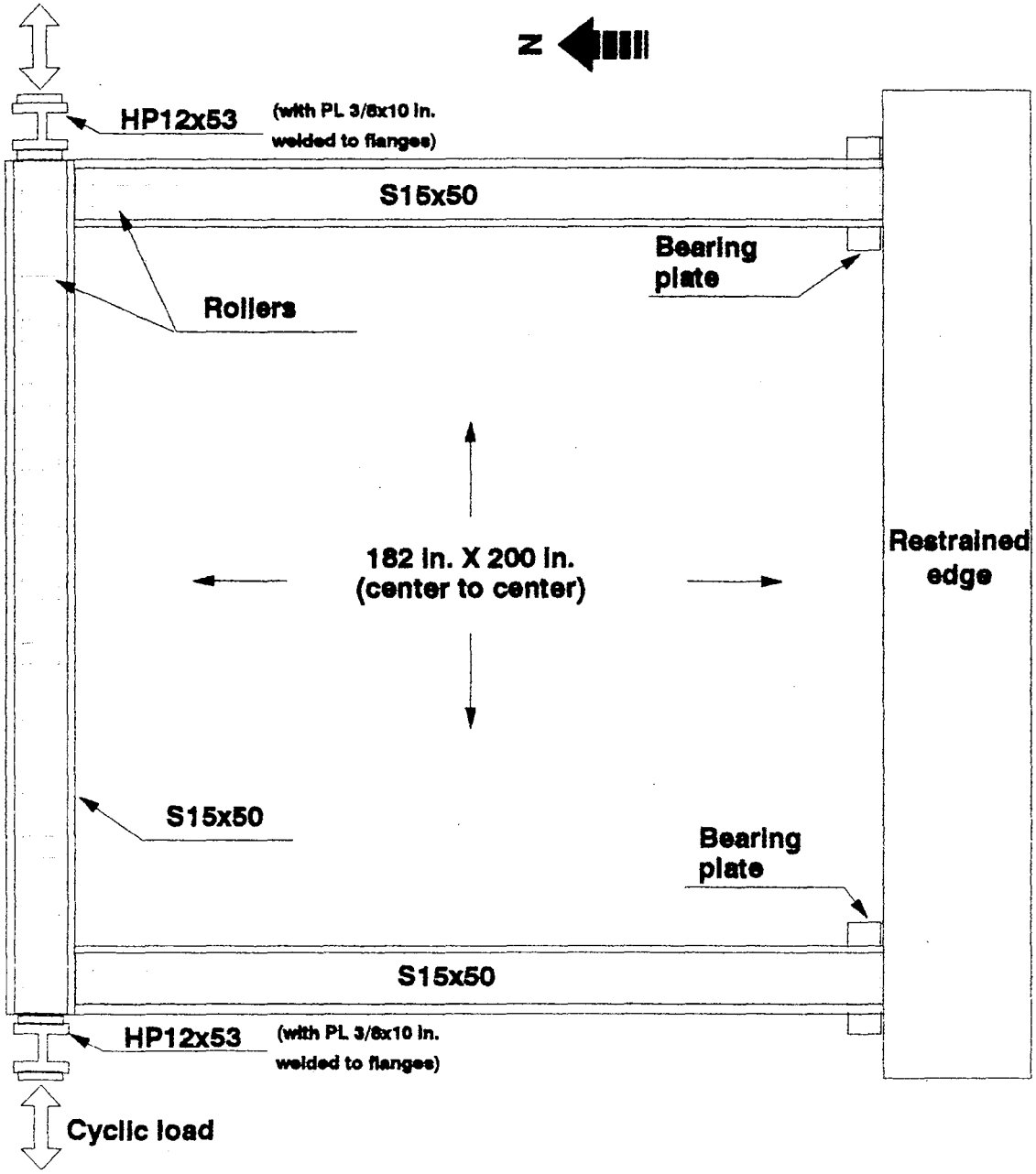

Figure 11. Schematic plan view of test frame

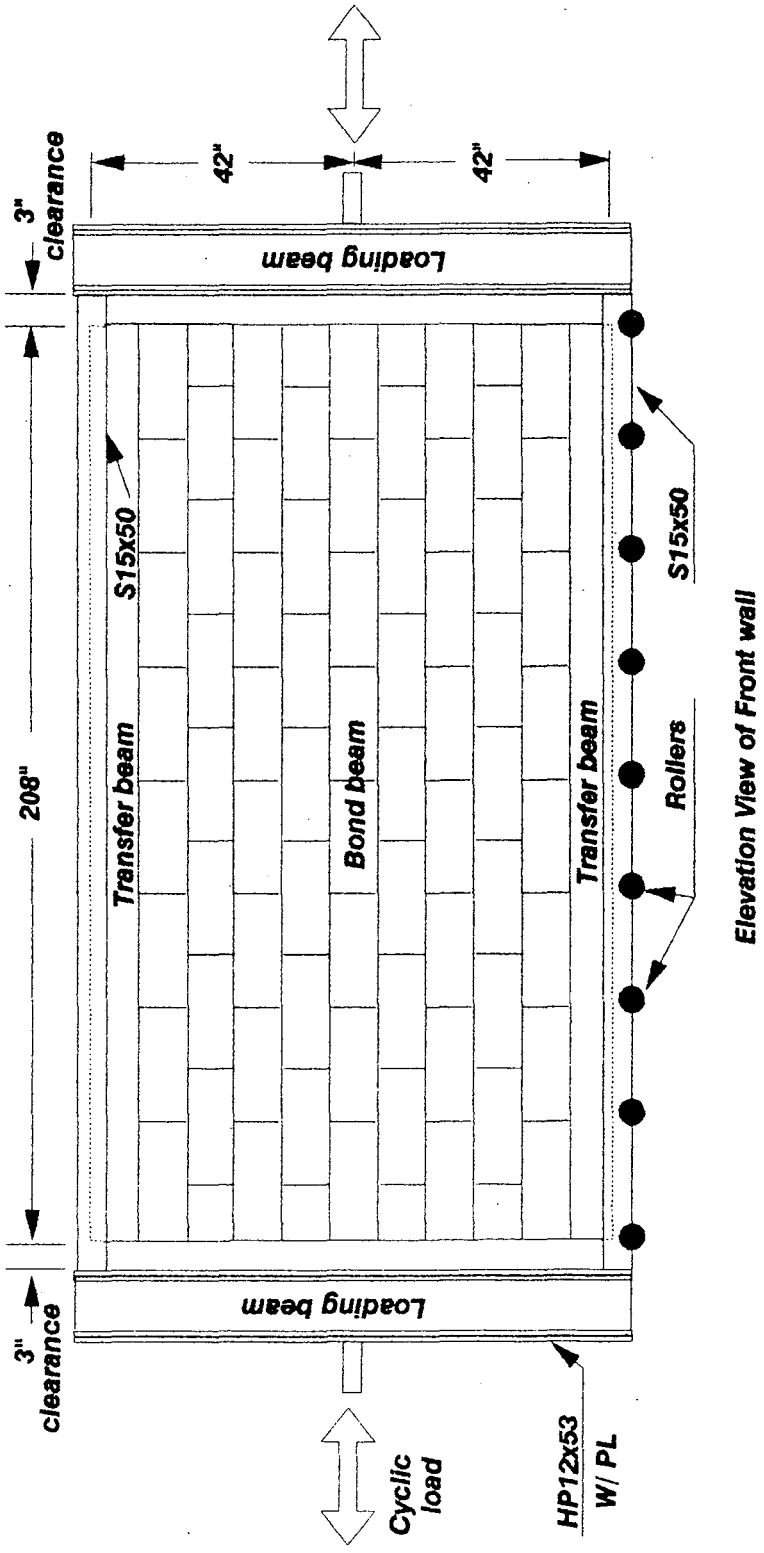

Figure 12. Front view of loading frame

Load was applied to the test frame through two double-acting hydraulic cylinders located at the ends of the front moving wall. The system is designed to carry a working load of $\pm$ 400 kips and a maximum displacement of $\pm$ 6.0 inches. Each of the hydraulic cylinders was mounted on two W36 x 230 anchored to the test floor.

A closed-loop MTS control system was used to control the displacement during the test. A direct current differential transducer (DCDT) was mounted on the front edge of the specimen and was used to deliver the feedback signal for displacement control. The loop was completed by a servo-valve which controlled the hydraulic actuators.

3.5.2. Data acquisition system and test instrumentation

3.5.2.1. Prisms An MTS hydraulic testing machine with a capacity of 640 kips in compression was used for applying compressive load to the prisms. Total vertical strains were measured on each face and over the entire height of the prisms using DCDT's. Figure 13 shows the instrumentation of the prisms.

3.5.2.2. Full-scale specimen Instrumentation was designed to determine the behavior of the system throughout the test. Three quantities were measured: forces, strains, and displacements.

Displacement measurements included relative displacements between the walls and the planks near the interface: interfacial slip, vertical separation, and out-of-plane separation. These displacements were measured with direct current differential transducers (DCDT's) and/or mechanical dial gages. Measurements were taken at each end and center points of each interface (above and below the floor). Relative horizontal displacements were measured between the top of walls and just above the interface. A DCDT was mounted near the mid-point of the floor's front edge and served to provide feedback to the MTS servo-controller. Absolute in-plane and out-of-plane displacements were measured at the outside face of the front wall, with reference to an auxiliary frame. Figures 14 and 15 show the placement of the DCDT's and dial gages, respectively.

Strain gages were attached to the vertical reinforcing steel bars in the walls to monitor the first yield and the distribution of the tensile strain in the vertical steel near the interface. Strain gages were also attached to the slab dowels to detect the change of tensile strain due to the edge zone stresses. Also, strain gages were attached to the webs of top and bottom steel loading beams to monitor the distribution of the axial strain to the bond beams. Some of the strain gages were destroyed during the construction stage of the specimen. Figure 16 shows typical strain gage arrangements for the vertical reinforcement in the walls and slab dowels.

Other data-gathering devices were used to record data during the test. These included a hand-held tape recorder, two cameras for taking photographs and slides, and a video camera to tape the testing as it progressed.

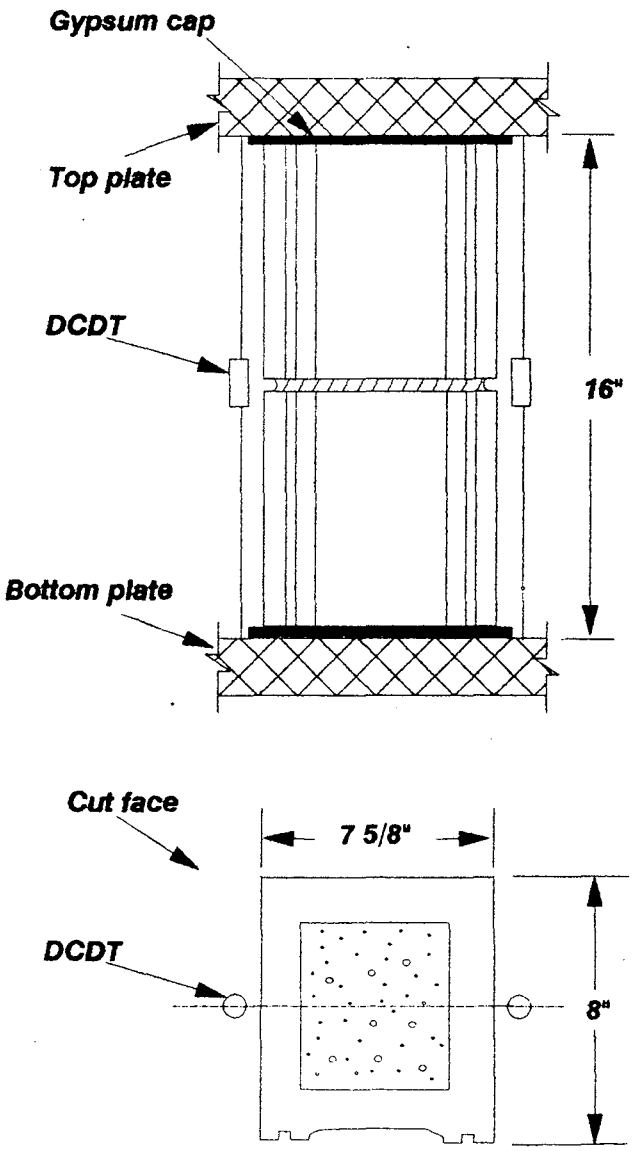

Figure 13. Prism instrumentation

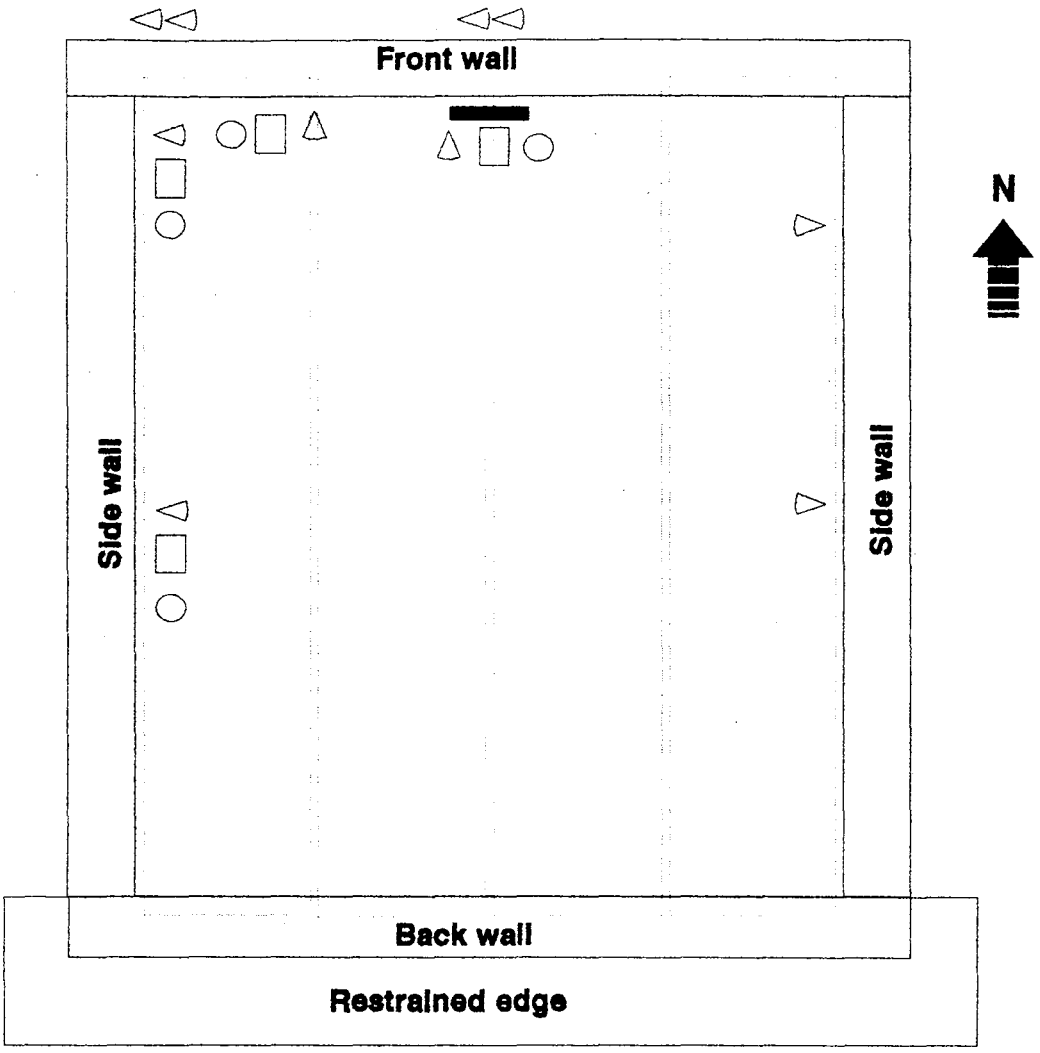

Figure 14. Placement of DCDT's

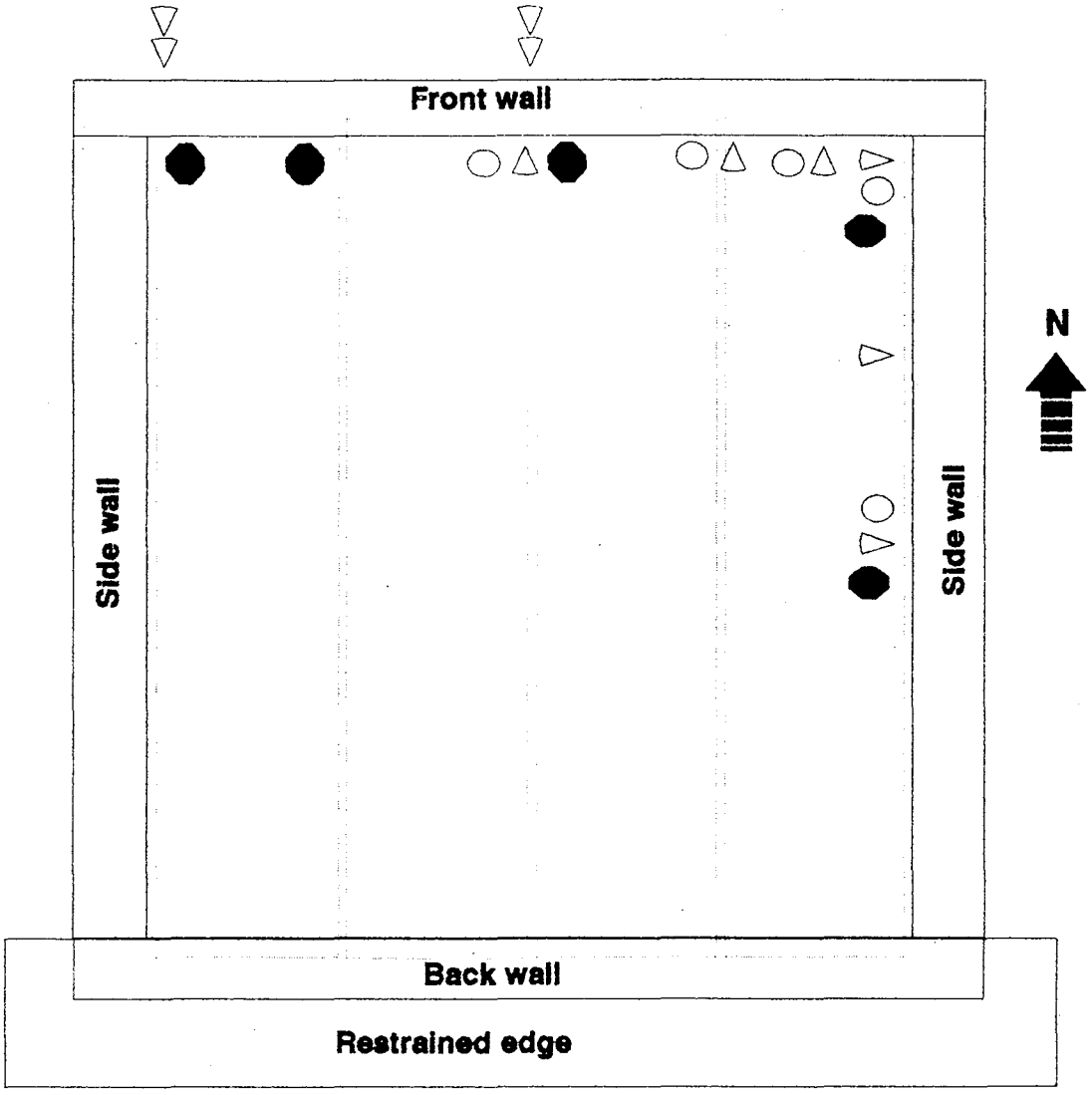

Figure 15. Placement of dial gages

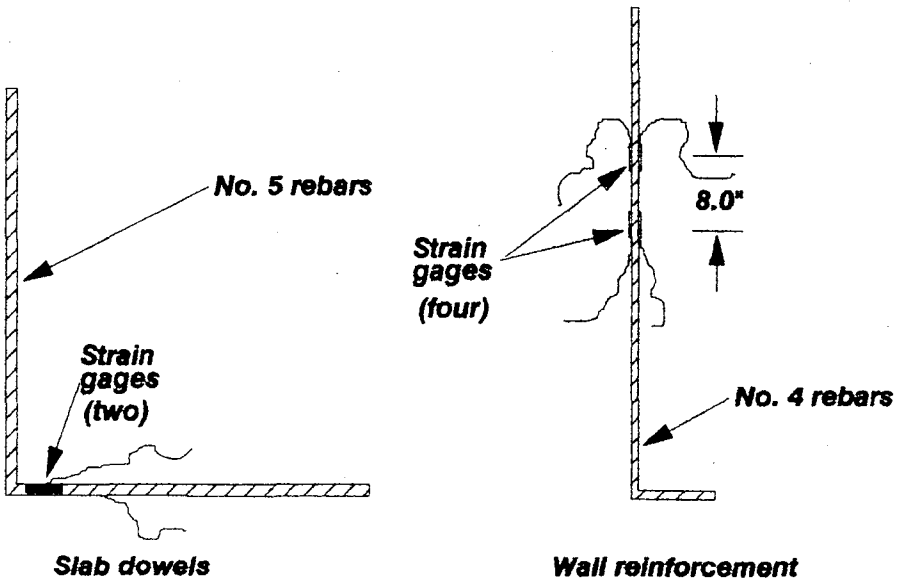

Figure 16. Instrumentation of vertical reinforcement in wall

All of the DCDT's, strain gages, and loading cells were monitored by the data acquisition system (DAS). The DAS consisted of 150 channel Hewlett Packard (HP) model 3497A data acquisition control unit interfaced with an HP model 85 microcomputer, a digital plotter, a dual disk drive, and five independent power supplies.

3.5.3. Load program

Sequential Phased Displacement (SPD) loading program was used for testing the specimen. The program employs a decaying loading cycle which establishes a correlation between demand and capacity for inelastic deformations [38]. This procedure utilizes standard stabilization cycles, beginning at approximately 0.0125 in. of displacement up to the first major event (FME). Once the FME occurred, a sequential phased displacement (SPD) loading procedure was followed. At each new displacement increment of loading after the FME, both decay and stabilization cycles were completed. The decay intervals were one-quarter the original displacement and followed by three or more stabilization cycles. If degradation of the final cycle was greater than five percent of the previous cycle, then additional stabilization cycles were required. Figure 17 shows a schematic plot of a typical SPD loading program.

The SPD procedure was used because it more accurately represented an earthquake excitation pattern than did the usual monotonic or simple reversed cyclic loading patterns. The TCCMAR have adopted this SPD loading program for most of its tasks. The rationale behind this approach centers on two main concepts: degrading in order to define the lower points within a given hysteretic curve, and finding a stabilized hysteretic curve.

4. TEST RESULTS

4.1. General

The results of the tests on the prisms and the full-scale specimen are presented in this chapter. These results are compared to the experimental results obtained from the previous task (Task 5.1) [11].

4.2. Compressive Strength of Masonry

4.2.1. Unit-mortar method

The ultimate compressive strength of the concrete block masonry at 28 days, f'_m, was determined by the Unit-Mortar Method described in UBC Section 2405 [37]. For type "S" mortar and using the average compressive strength of 3496 psi for the five units tested (8 x 8 x 16 in. two-cell hollow standard blocks), the value of f'_m obtained from Table 24-D of UBC Standard S2405 [37] was 1875 psi.

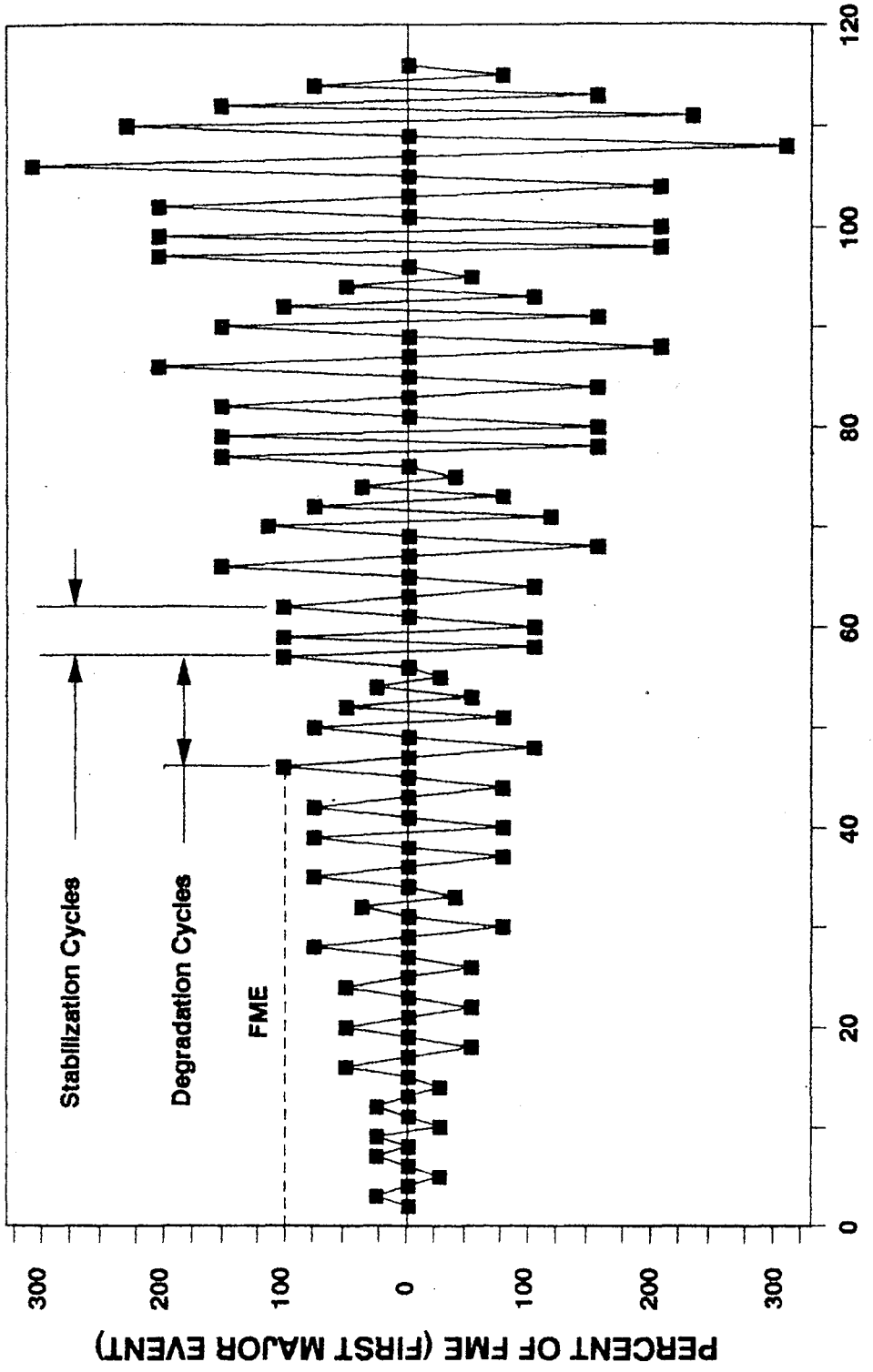

Figure 17. Typical SPD loading program [38]

4.2.2. Prism test method

The Prism Test Method for determining f'_m is outlined in the ASTM Standards, E 447-80 [36]. Table 6 gives a summary of the prisms tested. Since all prisms were two blocks high, the correction factor for the h/t ratio was equal to one. The compressive strength, f'_m, was 3754 psi and 2357 psi for grouted and ungrouted prisms, respectively. For the grouted prisms f'_m is mostly controlled by the strength of the grout.

All grouted prisms failed in shear and exhibited similar behavior, with diagonal cracks crossing both the grout and the block, or crushing occasionally. The higher compressive strength and modulus of elasticity of the grout as compared to those of the block units resulted in the grout resisting the majority of the load and controlling the axial and lateral deformation. The deformation was larger in the block units compared to the grout, but this did not cause pressure on the face shells of the units. The prisms crushed or cracked diagonally once the compressive strength of the grout was exceeded. This failure was sometimes followed by partial separation of the grout from the units at failure. In general, the faceshells did not split off the grout cores.

The ungrouted prisms generally failed by tensile splitting occurring first on the sides, and then spalling of the face shell. The ungrouted prisms produced an average compressive strength that is 37% lower than the grouted prisms.

4.3. Stress-Strain Relationship

Figure 18 shows the stress-strain relationship obtained for grouted concrete masonry prisms. Because the walls were fully grouted, stress-strain relationship of the ungrouted prisms was not of concern, only the ultimate load was reported. Strain measurements were taken up to approximately 90 percent of the maximum load due to sudden explosive nature of the failure which dictated the removal of the measurement devices to avert damage. Although the measurement devices were removed, the test data indicated that the relationship for stress versus strain changed from linear to non-linear near the ultimate stress. From a linear analysis of the data, the modulus of elasticity was 445 f'_m (1660 ksi).

4.4. Full-Scale Specimen

4.4.1. Test synopsis

4.4.1.1. Diaphragm The specimen consisted of four planks oriented transversely to the direction of the applied load. This test specimen will be referred to as Test C for comparison purposes. All sides of the diaphragm were connected to the walls by slab dowels embedded in the topping and run through the cores of the masonry units. There were twelve dowels (No. 5 reinforcing bars) per side, equally spaced. The concrete of

Table 6. Summary of compressive strength of concrete masonry, f'_m

Specimen Type	Ultimate Load (kips)	Compressive Strength, f'_m (psi)	
		Gross Area	Avg. Net Area
Grouted Prisms (cut)	208.8	3356	3421
	210.1	3294	3357
	201.0	3186	3247
	220.7	3531	3599
	256.6	4121	4200
	244.6	3903	3978
	239.2	3863	3938
	282.8	4206	4287
	Average	3683	3754
Ungrouted Prisms	105.0	(premature failure)	
	146.9	1233	2309
	154.9	1300	2435
	148.0	1242	2327
	Average	1258	2357

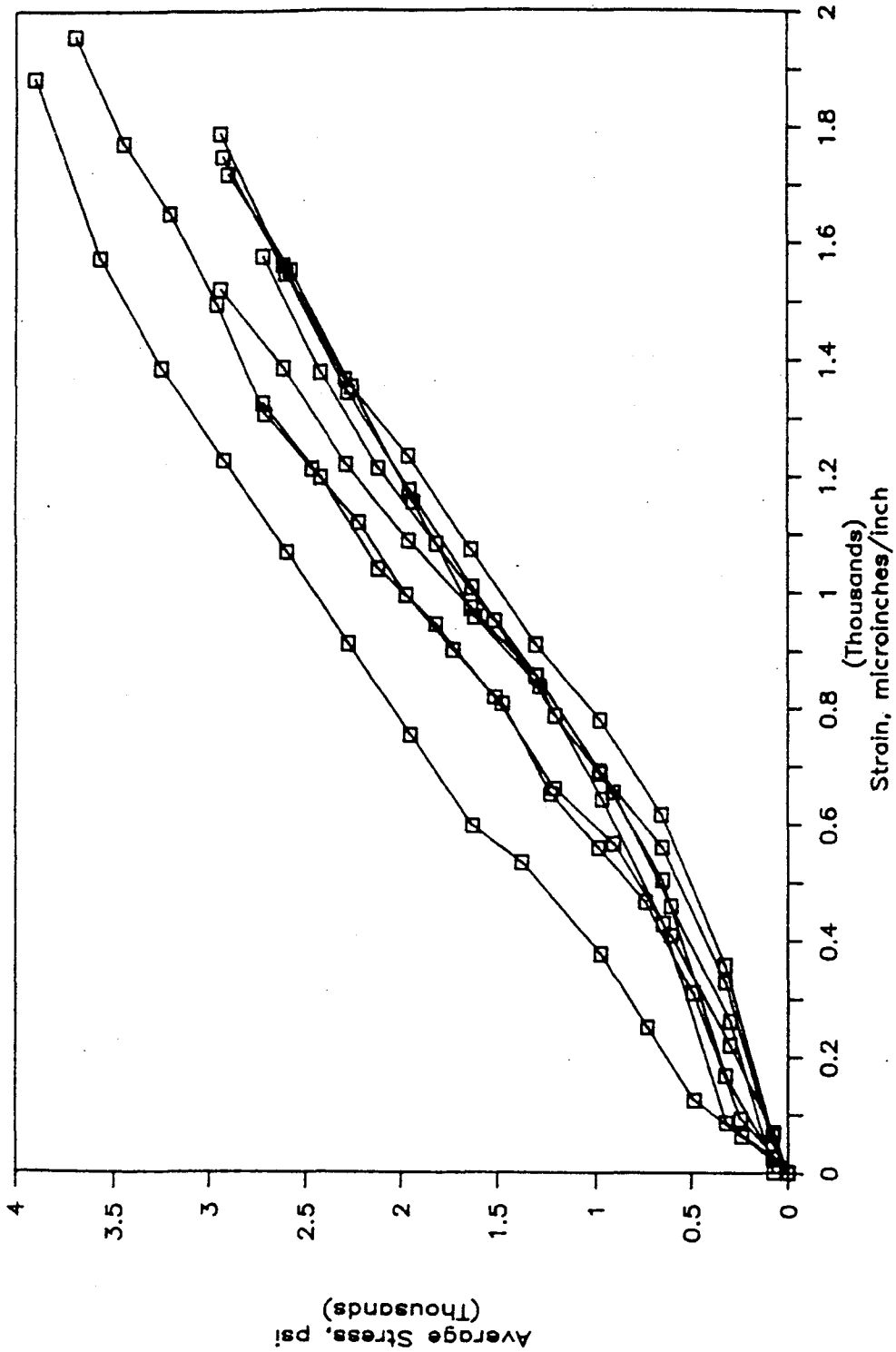

Figure 18. Stress-strain relationship for grouted prisms

the topping penetrated inside the seams of planks. The compressive strength of the concrete used was 7233 psi. The strength of the span-deck plank was 8300 psi, based on typical plant cylinder tests.

The test was performed under the guidelines of the SPD loading procedure. Displacement increments of 0.025 in. through 3.5 in. were used as shown in Figure 19. The first major event (FME) was encountered at load point 120 at a measured displacement of 0.31 in. east and a load of 270.8 kips. The failure was a diagonal crack in the planks extending from the southeast corner to near the northwest corner. This type of failure was designated as a "diagonal tension" failure. This event was recorded as a discontinuity on the hysteretic curves for the 0.375-in. cycles as shown in Figure 20. This was accompanied by few cracks in the planks near the support beam due to cantilever action. These cracks continued to propagate throughout the test. Figure 21 shows the crack pattern for the diaphragm.

The load began to decrease thereafter at higher displacement increments. This load, 270.8 kips, was considered to be the ultimate load attained for this specimen. At a load of 249.0 kips (0.31 in. west, displacement), a few more cracks, parallel to the loading wall, occurred in the planks near the support. At approximately 0.5 in. displacement, floor cracks began to propagate from the back toward the loaded edge, parallel to the east side wall and approximately 2 ft. away from it. These cracks coincided approximately with the termination point of the slab dowels embedded in the topping. Similar cracks occurred near the west side wall. As the test proceeded, these cracks began to propagate toward the front loading wall and they increased in width as the displacement increased.

At a displacement of 2.00 in. (load point 305), two 2-ft. square portions of concrete had fallen to the floor making it possible to briefly inspect the bottom face of the diaphragm for crack occurrence. Most of the cracks penetrated through the full depth of the planks. In addition, the concrete had begun to spall around the exterior prestressing tendons of the exterior planks some time during the test. Extensive cracking of the restrained end edge zone was noted at higher displacement magnitudes, almost causing total separation of the diaphragm from the support beam. These cracks were located at the end of the grout that was placed in the cores of the planks to be used for connecting the specimen to the supporting beam.

Figure 22 shows the load and displacement histories for the test specimen. The upper graph plots load point versus displacement, whereas the lower graph displays load point against virgin and stabilized loads (first and last cycles of a specific displacement increment, respectively).

4.4.1.2. Connection The connection between masonry walls and diaphragm was constructed following the in-field practice of masonry construction. That is, connecting the walls to plank diaphragm by means of slab dowels embedded in the concrete topping

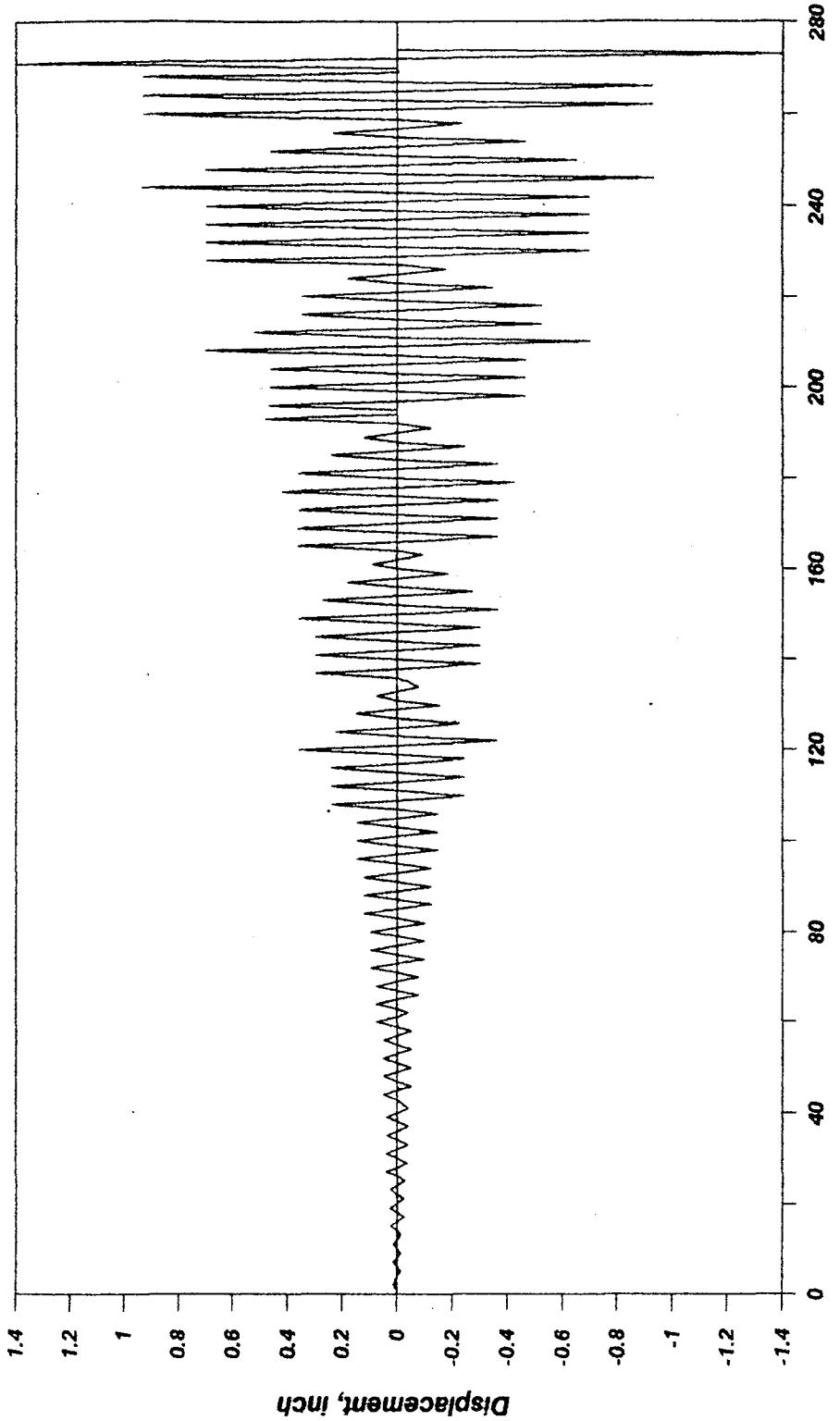

Figure 19. Load program for Test C

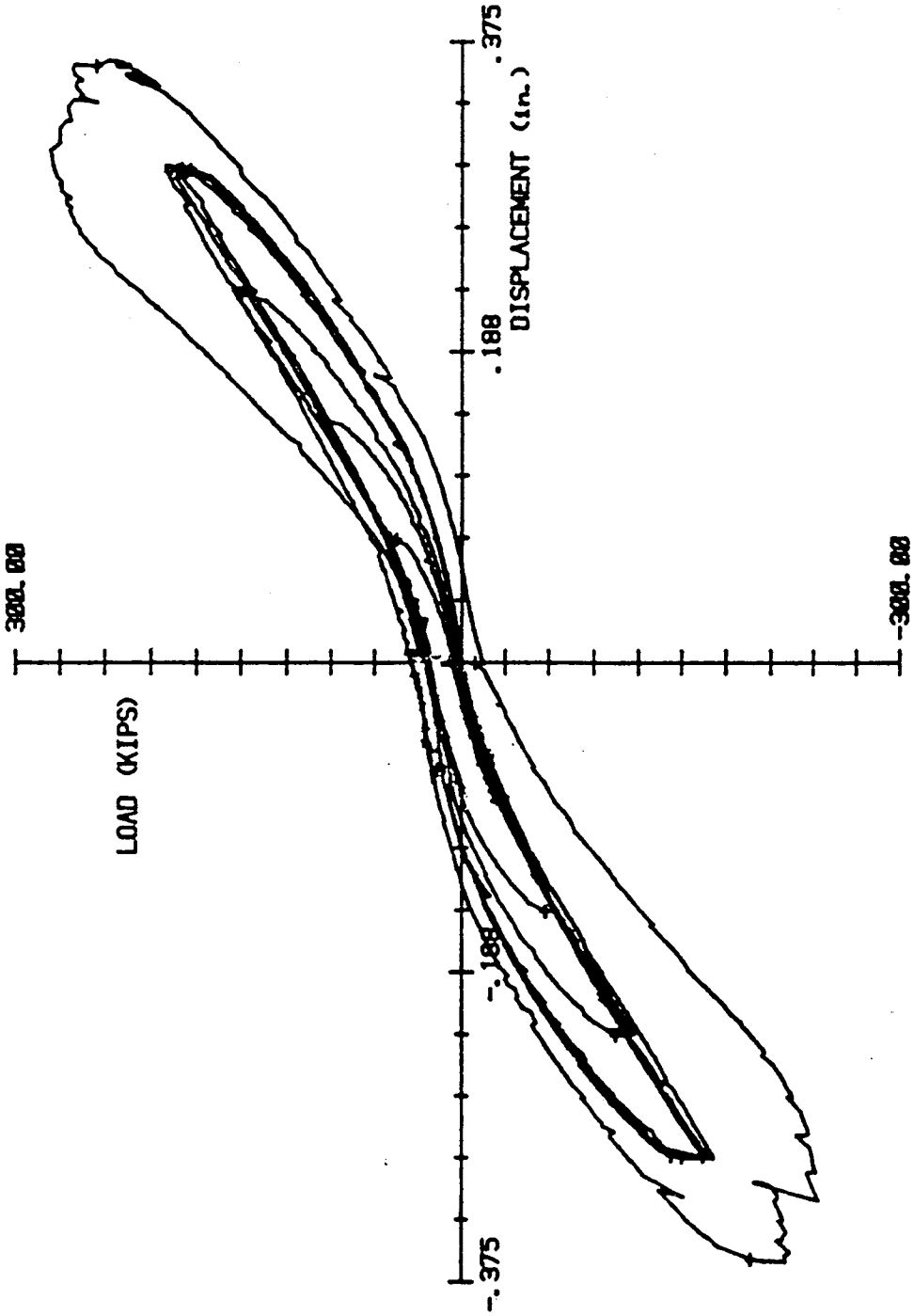

Figure 20. Hysteretic curve for Test C

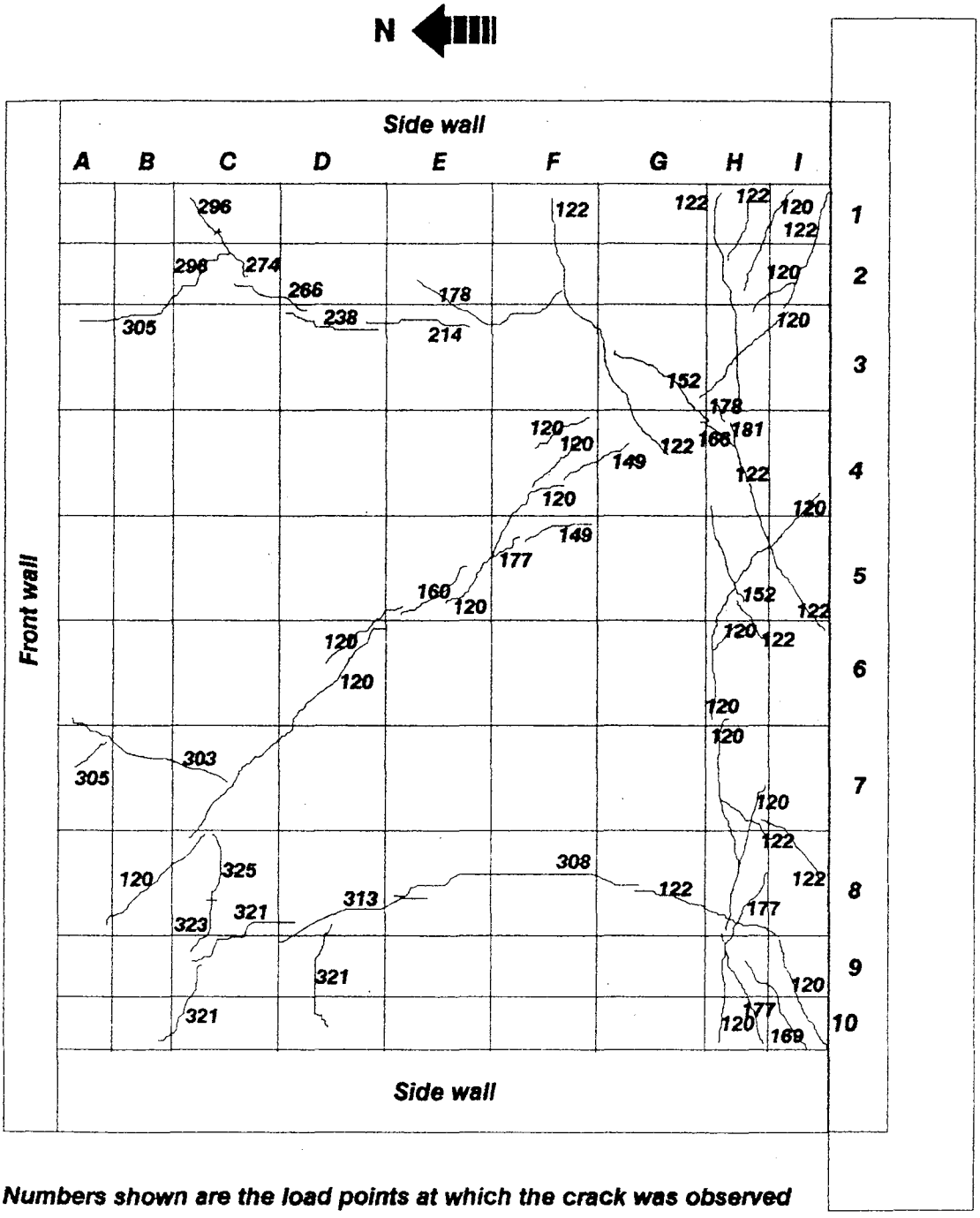

Figure 21. Diaphragm crack pattern for Test C

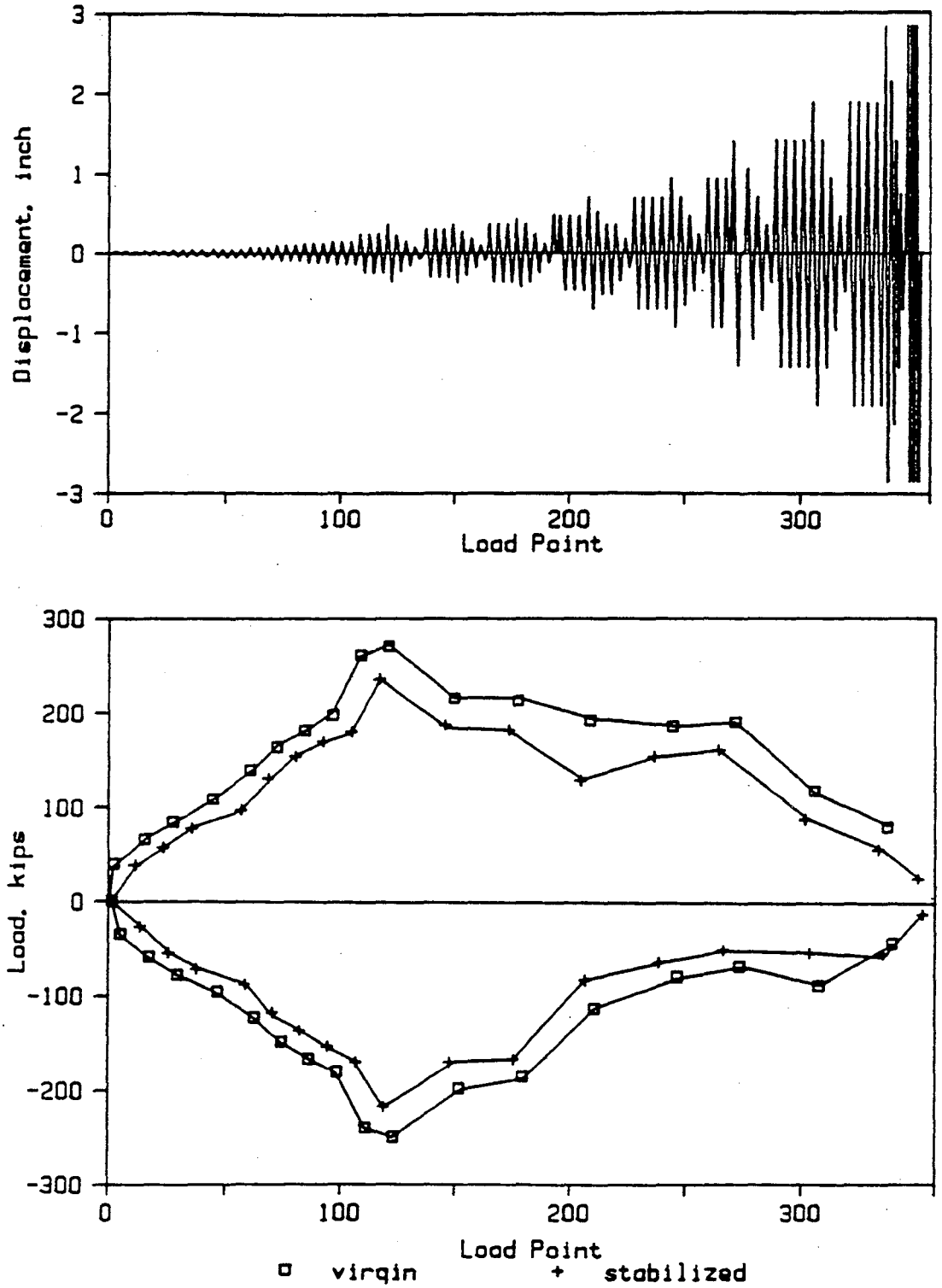

Figure 22. Displacement history and virgin/stabilized loads for Test C

(when used) and extended inside the cores of the masonry blocks of the walls. Two types of connection details were used: 1) floor-to-side/front walls (see Sections A-A and C-C of Figure 5), and 2) floor-to-back walls (see Section B-B of Figure 5).

Recordings were taken for slip between the walls and the floor as well as vertical and out-of-plane separations. This was monitored by DCDT's and mechanical dial gages. When the diagonal tension crack occurred across the floor (load point 120), a noticeable change in slip of side and walls relative to floor was observed.

After the FME occurred, the transverse cracks near the south (restrained) edge began to propagate toward and parallel to the side walls. These cracks were located at about 2 ft. from the interface indicating the termination point of the slab dowels embedded in the topping. Similar cracks appeared near the front wall at load points 274 and 321 with associated displacements of 1.5 in. (191.0 kips) and 2.0 in. (89.3 kips), respectively. These failures were considered to be directly related to the connection details. The cracks continued to extend and widen throughout testing. Figure 23 shows schematically the crack pattern near the interface and around the perimeter of the specimen.

As the displacement increment increased, few cracks originated from the boundary cracks and began to propagate toward the interface region perpendicular to the walls and in between the slab dowels. The dowels were equally spaced at 16 in. These cracks penetrated through the full depth of the slab. Figures 24 and 25 show the plots of average stress in the slab dowels, located at interface midpoint of side wall and about 35 in. from the west edge of front wall, versus load point number throughout the test. The rest of the strain gages placed on the slab dowels were badly damaged during construction, therefore, no other data were recorded.

During the inspection of the bottom face of the diaphragm, two cracks were observed on the exterior edges in the lower wythe of the outer planks. Pieces of concrete had fallen to the floor at those locations. That was due to the high strains in the prestressing strands exceeding the ultimate strain of the surrounding concrete.

4.4.1.3. Walls The walls were fully grouted and reinforced to ensure initial failure in the diaphragm slab or connection. Few cracks appeared in the front wall during testing. First crack occurred at a load point 82 (0.10 in. west, and load of 136.4 kips), about 3.5 ft. from the bottom east corner of wall. At load points 84 and 92, (0.125 in. displacement cycles and loads of 181.0 kips and 170.6 kips, respectively), the crack extended to the third course from the base following a stepped path along the bed and head joints of masonry blocks, simultaneously, and moving toward the east side of wall. This crack was accompanied by another crack which started at 4.5 ft. from the same corner and extended to the second course. Figure 26 shows the crack pattern of the front loading wall.

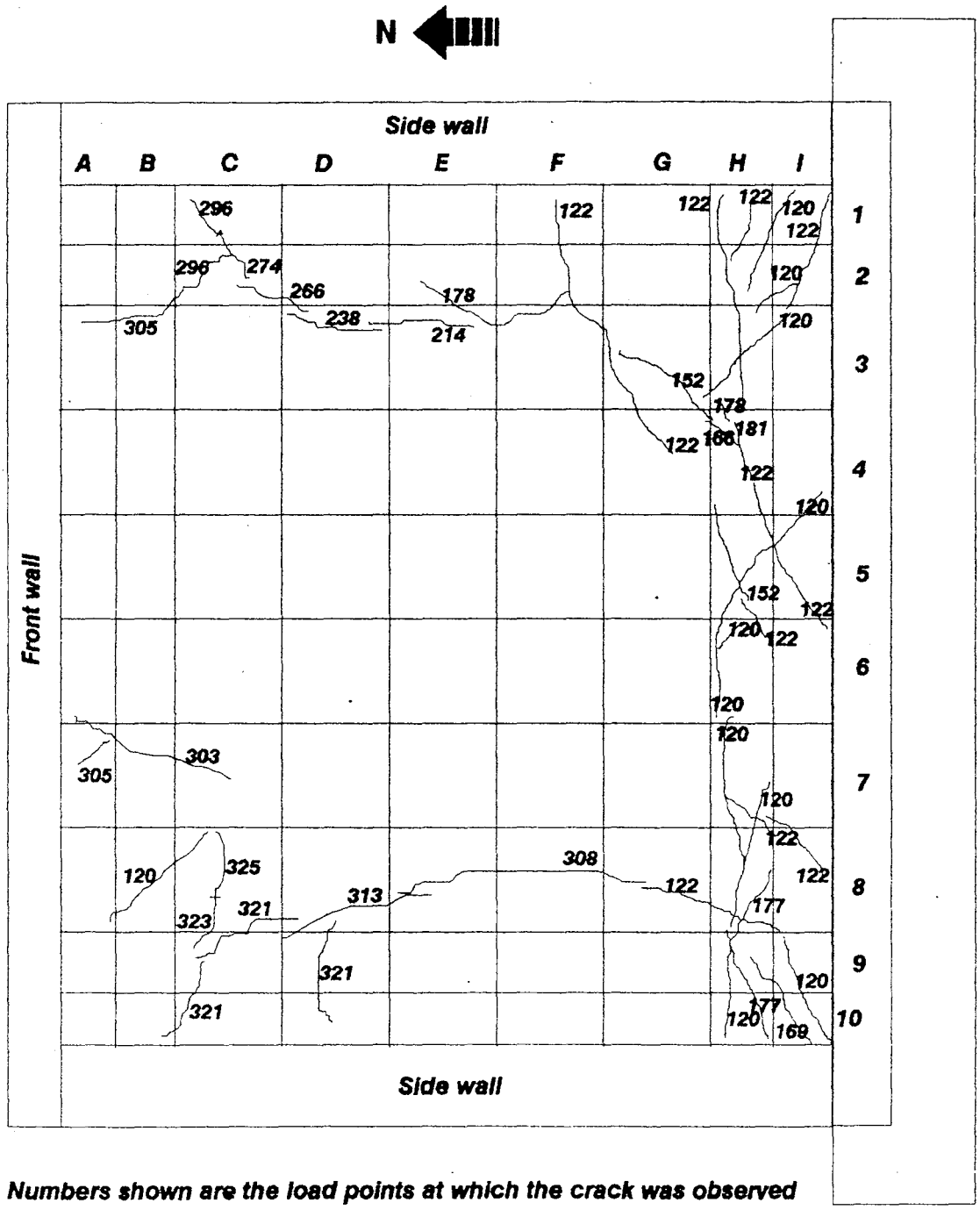

Figure 23. Interface crack pattern of Test C

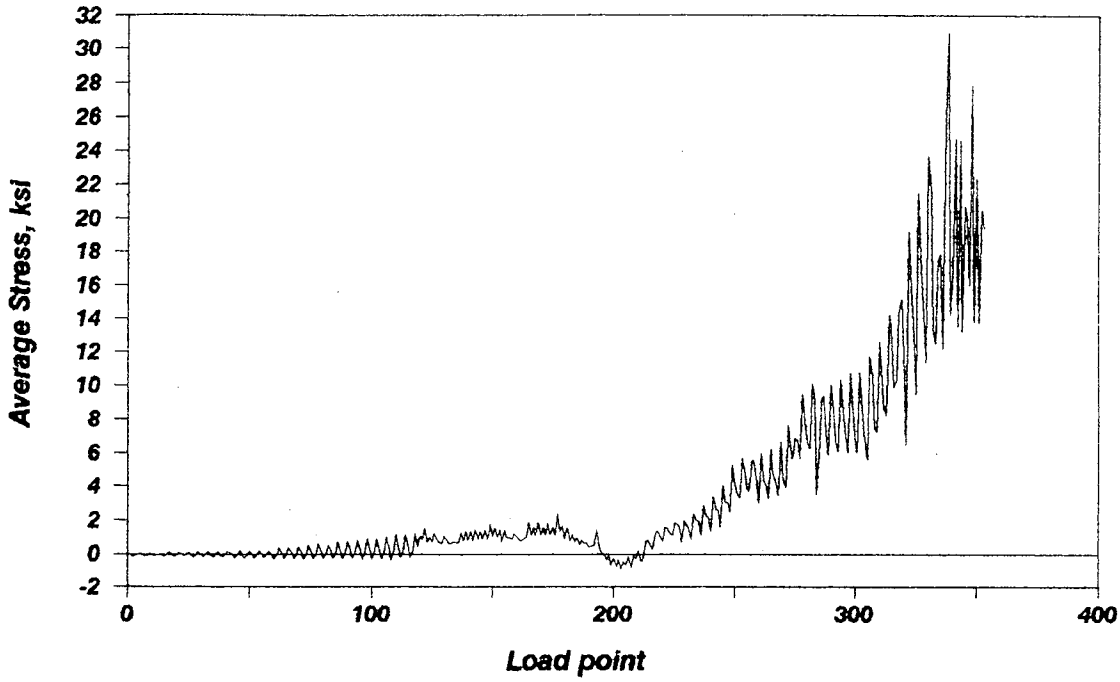

Figure 24. Tensile stress in slab dowels at 35" from west edge of front wall

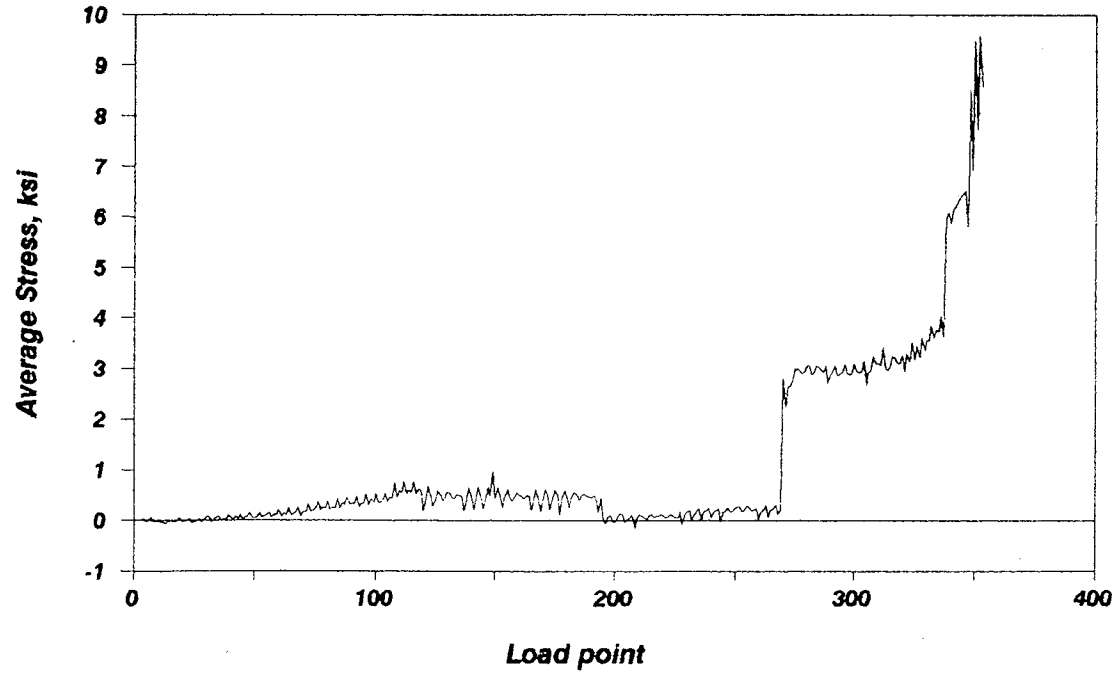

Figure 25. Tensile stress in slab dowels at midpoint of side wall

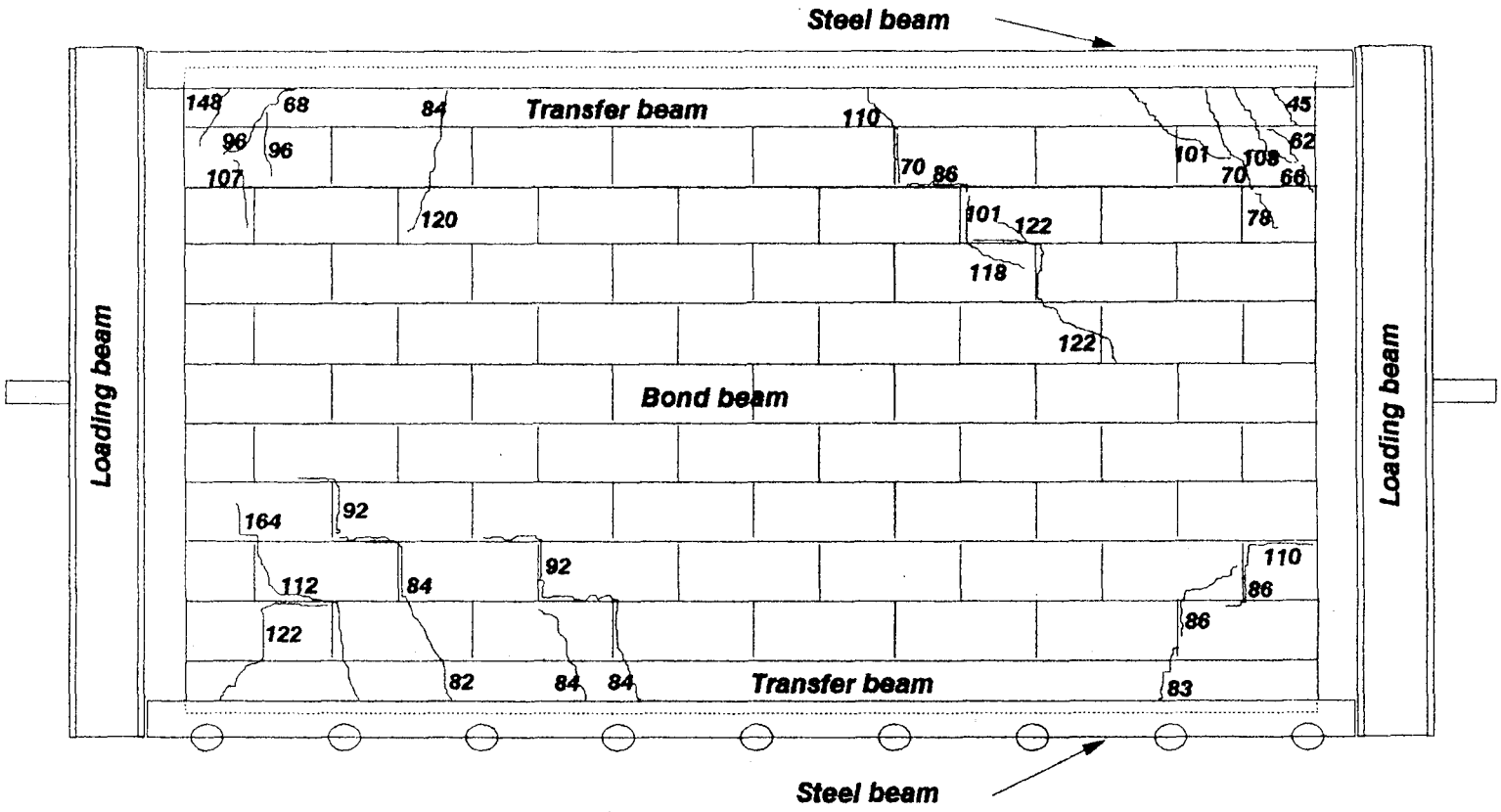

Numbers shown are the load points at which the crack was observed

Figure 26. Crack pattern of front wall

At the 0.125 in. displacement and a load of 166 kips, another crack initiated at about 4.5 ft. from the top west corner and extended, during a displacement of 0.14 in. and a load of 143 kips (load point 101), to the third course from the top at an approximately 45° angle.

At a displacement of 0.15 in. and a load of 166 kips, another crack initiated at about 4 ft. from the top west corner and extended, during a displacement of 0.25 in. and a load of 202.0 kips (load point 118), to the third course from the top at an approximately 55° angle with respect to the horizontal. This crack was followed by another crack, starting at floor level and about 2 ft. from the west edge of the wall and extending toward it, after the diagonal crack had occurred in the diaphragm, at load point 122 with a displacement of 0.325 in. corresponding to a load of 249.0 kips. These cracks did not increase in width nor in length throughout testing. All other cracks in the front wall were very minor and had initially occurred due to the shear studs that were used in the top and bottom bond beams of wall to transfer load from loading frame to specimen.

Regarding the side walls, there was no noticeable crack occurrence until reaching the higher displacements. At 2.00 in. displacement and larger, and when the cracks in floor diaphragm near the interface started extending toward the walls perpendicularly, vertical cracks were observed at approximately 2 and 4 ft. from the front edge in both walls.

At a displacement of 0.5 in. with a load of 203.0 kips, two cracks appeared in the back wall, one on either edge of wall. These cracks extended from the top bond beam to the floor level, and at about 4 ft. from the corners at an approximately 55° angle with respect to the horizontal. Also, the back corners that connect the side walls to the back wall had split vertically due to the cantilever action. These cracks increased in width, as displacement was increased, which caused a significant out-of-plane movement of specimen. The width of these cracks widened to 3/4 in., approximately, at the end of the test run.

4.4.2. Previous tests

4.4.2.1. Test A (Test #13 of Task 5.1) The specimen consisted of four planks oriented with the seams perpendicular to the loading beam. The planks were supported by steel beams. The planks were 8 in. thick and covered with a nominal two-in. concrete topping cast in place. The compressive strength of the topping was approximately 5100 psi while the strength of the plank was assumed to be 8300 psi (based on typical plant cylinder tests).

The planks were connected to the supporting steel beams by means of shear studs, 5 in. long and 3/4 in. in diameter, on all four sides around the perimeter of the edges. Three studs were placed in each void at the ends of each plank whereas the longitudinal edges incorporated only two studs per void.

The FME occurred as a result of a diagonal tension crack extending across the diaphragm from the northeast to the southwest corners (see Reference 11 for details). The displacement at which the FME occurred was 0.15" with and a load of 230.4 kips. A similar crack from the southeast corner to the northwest corner occurred when the displacement was reversed. Other diagonal cracks continued throughout the test run. The ultimate load of 295.6 kips was recorded at 0.5 inch displacement.

4.4.2.2. Test B (Test #14 of Task 5.1) This test was similar to Test A except that the planks were oriented with the seams parallel to the applied load. The compressive strength of the 2-in. concrete topping was 4900 psi (the compressive strength of planks was assumed to be 8300 psi).

The FME occurred at a displacement of 0.15 in. west with a recorded load of 260.8 kips. This major crack was a diagonal tension crack extending across the northeast to southwest corners. Similar diagonal crack across the planks occurred when displacement was reversed. Maximum load of 302.0 kips was achieved at 0.44 in. displacement.

4.4.3. Comparison of diaphragm results

Test C can be compared to Tests A and B. All of these tests consisted of 8-inch planks and 2-inch topping. Test C and Test A planks were oriented in the north-south, while Test B planks were oriented in the east-west direction. The orientation of the planks were found to have negligible effect on the behavioral characteristics of topped diaphragms [11]. Therefore, both tests (A and B) can be used for comparison purposes. The frame used for Tests A and B consisted of steel sections, while the frame used for Test C consisted of masonry walls.

Figure 27 shows the cyclic stiffness comparison of the three tests. The cyclic stiffness for Test C was lower than that for Tests A and B up to 0.75-inch displacement. This can be attributed to the lower stiffness of the masonry wall frame as compared to the steel frame. After the 0.75-inch displacement the stiffness of all three tests was essentially the same.

Figure 28 shows the envelope curves comparison of the three tests. The peak load was similar for both Tests A and B, but slightly lower for Test C. The lower value of the peak load for Test C is attributed to the failure of the connection between the side and the back walls.

The behavior of the diaphragm in all tests was quite similar. All slabs failed in diagonal tension with the exception that the slab of Test C had only one diagonal crack indicating unsymmetry in its hysteretic behavior. The initial stiffness for Test A and B was 2698 and 3298 kips/in., respectively; while Test C yielded an initial stiffness of 3064 kips/in.

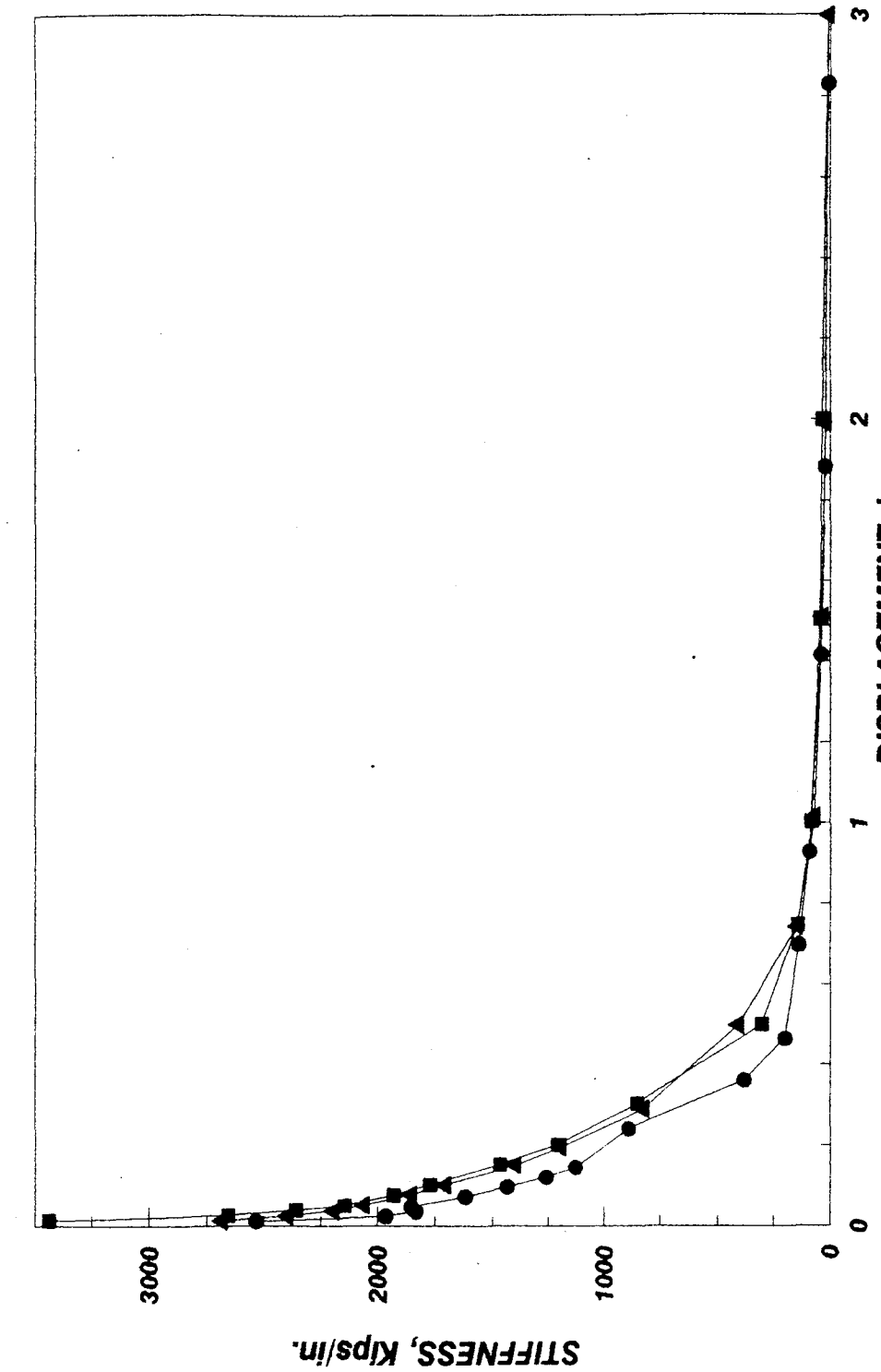

Figure 27. Stiffness comparison for Tests A, B and C

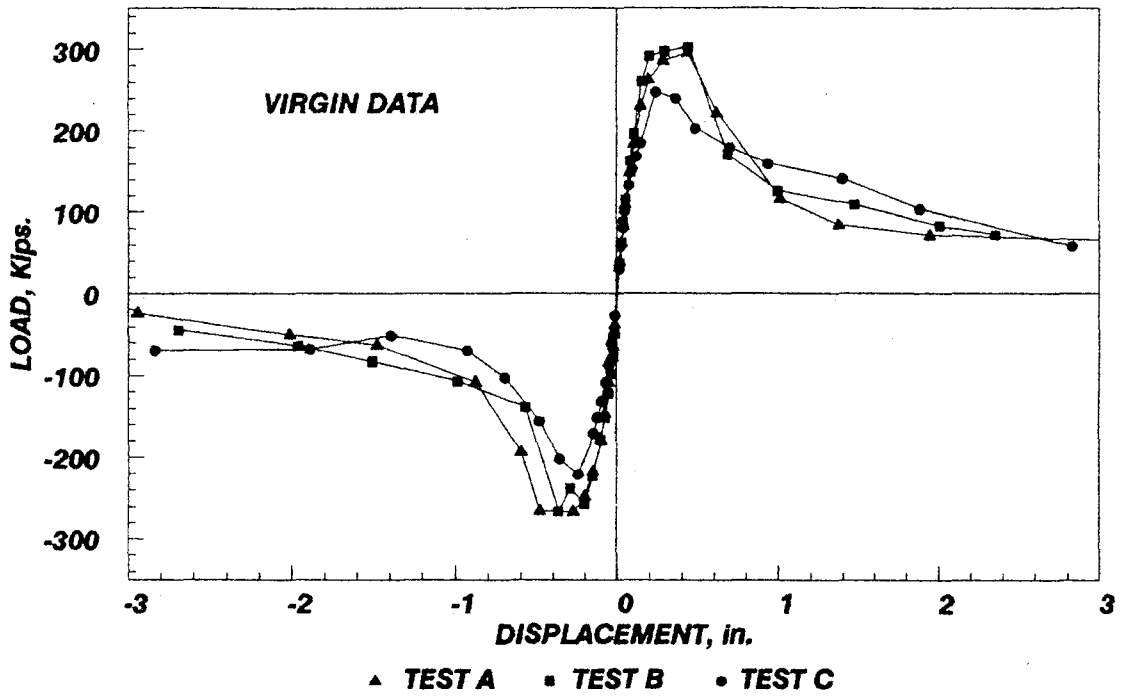

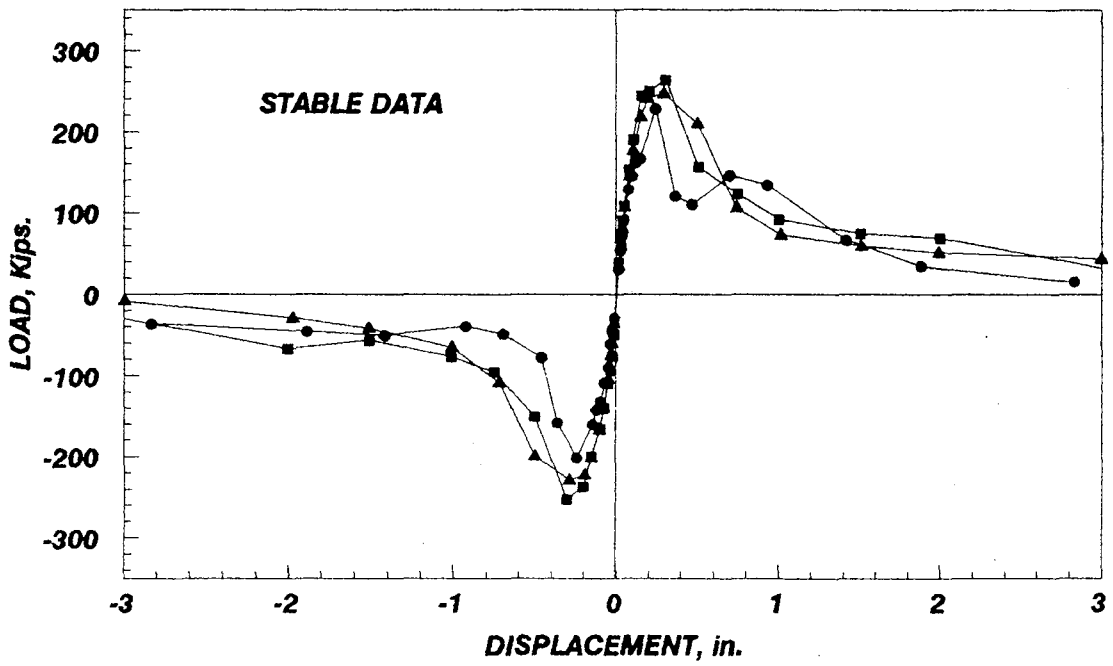

Figure 28. Envelope curve comparison for Tests A, B and C

The FME and peak load values of all three tests are listed in Table 7 with their associated displacement values. The FME of Test C occurred at higher displacement (0.31 in.) than those of Tests A and B (0.15"), but with comparable values. The peak loads of Tests A, B, and C were reached at displacements of 0.43, 0.44, and 0.31 in. with corresponding load values of 296, 302, and 271 kips, respectively.

Table 7. Comparison of FME and Peak Loads

Test #	FME (kips)	Displacement (in.)	Peak (kips)	Displacement (in.)
A	230	0.15	295.6	0.43
B	261	0.15	302.0	0.44
C	271	0.31	270.8	0.31

5. ANALYTICAL INQUIRY

5.1. General

The analytical expressions derived for the diaphragms in Task 5.1 [11] were used to determine preliminary predictions for the FME, the peak load and the initial stiffness. A short summary of these expressions is presented in the next sections.

5.2. Initial Stiffness Prediction

The initial stiffness consisted of four components:

$$K_{tot}=\frac{1}{(\frac{1}{K_b}+\frac{1}{K_s}+\frac{1}{K_z}+\frac{1}{K_f})} \qquad (5\text{-}1)$$

where:

K_{tot} = diaphragm initial stiffness, Kips/in
K_b = bending stiffness component, Kips/in
K_s = shear stiffness component, Kips/in
K_z = edge zone stiffness component, Kips/in
K_f = framing members stiffness component, Kips/in

5.3. First Major Event Prediction

Based on the orientation of the planks, the FME is the smaller of the following two predictions. These are the shear-bond failure and the diagonal tension mode equations as shown by Equations [5-2] and [5-3], respectively.

The shear-bond failure mode is given by:

$$V_{FME}^{P}=\frac{T'_{av}d_g l_s(b+l''_p)}{ar_5} \qquad (5\text{-}2)$$

where:

V^P_{FME} = predicted FME for shear-bond failure mode, Kips.
T'_{av} = average seam shear stress from elemental tests, Ksi.
d_g = grout penetration depth, in.
l_s = length of the seam, in

a = length of the diaphragm in the north-south direction, in.
b = length of the diaphragm in the east-west direction, in.
r_s = constant (Refer to Reference 11)
l''_p = constant (Refer to Reference 11)

The diagonal tension failure mode is given by:

$$V^P_{FME}=3.3\sqrt{f'_c}bd+N_{cp}\frac{d}{4l_w} \quad (5\text{-}3)$$

where:

V^P_{FME} = predicted FME for diagonal tension failure mode, lbs.
f_c' = concrete compressive strength, psi.
b = width of diaphragm, in.
d = effective plank depth, in.
N_{cp} = normal prestressing force, lbs.
l_w = effective diaphragm width (0.8 b), in.

5.4. Peak Load Prediction

The peak load is the lowest of that predicted by the shear-bond failure and diagonal tension modes as shown by Equations [5-4] and [5-5], respectively.

The shear-bond equation is:

$$V^P_{LS}=\frac{5.5n+0.9(N_c+N_t)}{(\frac{b}{2}-w+b''+a)}(b+l'_p) \quad (5\text{-}4)$$

where:

V^P_{LS} = predicted limit state load for shear-bond failure, Kips.
n = number of weld ties
N_c = compressive resultant force between planks
N_t = tensile resultant force between planks
b = width of diaphragm, in.
w = width of individual planks (4 feet in this study), in.
b" = edge zone distance, in.
a = length of diaphragm, in.
l_p' = constant (refer to Reference 11)

and the diagonal tension equation is:

$$V_{LS}^{P}=3.3\sqrt{f_c'}bd+N_{cp}\frac{d}{4l_w} \qquad (5\text{-}5)$$

where

V^P_{LS} = predicted FME for diagonal tension failure mode, lbs.
f_c' = concrete compressive strength, psi.
b = width of diaphragm, in.
d = effective plank depth, in.
N_{cp} = normal prestressing force, lbs.
l_w = effective diaphragm width (0.8 b), in.

5.5. Comparison with Experimental Results

The initial stiffness, FME and peak loads were calculated using the equations presented earlier. The results of these equations is compared to the experimental data as shown in Table 8.

Table 8. Comparison of Experimental and Analytical Results

	Experimental	Analytical
Initial Stiffness, Kips/in	3064	3054
First Major Event, Kips	271	240
Peak Load, Kips	271	246

6. SUMMARY, CONCLUSIONS AND RECOMMENDATIONS

6.1. Summary

This investigation on the behavioral characteristics of hollow-core planks subjected to in-plane shear loading was part of the overall Masonry Building Research Program being supported by the National Science Foundation and coordinated by the Technical Coordinating Committee on Masonry Research. Three full-scale plank diaphragm tests were reviewed as part of the investigation of the supporting members and connection detail parameters. Two of these tests were built and tested previously during task 5.1 in which the planks were supported by steel beams and connected by means of shear studs. The third test was designed, built, and tested during this phase of the project. The specimen consisted of a plank diaphragm supported by and connected to reinforced concrete masonry walls, instead of steel beams, and was constructed by professional masons, complying with the in-field practice.

The main objective of this study was to determine the effects of stiffness change of diaphragm supporting members, as well as their connection type, on diaphragm strength and behavior due to in-plane cyclic loading. Basic properties of interest included stiffness, ultimate load, failure mode and hysteretic behavior.

The specimen was subjected to displacement controlled in-plane shearing of the front edge while the back edge is maintained fixed. The procedure involved reversed cyclic loading known as "Sequential Phased Displacement" (SPD) representing an earthquake excitation pattern rather than an ordinary monotonic or simple reversed cyclic loading pattern.

Quantities of prime interests, namely, loads and displacements were continuously recorded. Load-displacement curves for all displacement increments were plotted. The failure mechanism and cyclic behavior were carefully studied and compared to previous tests. The test results, along with previous results, were compared with the analytical results.

6.2. Observations and Conclusions

The following conclusions were based on the results of the investigation summarized above.

1. The initial stiffness of specimen with masonry walls was 14 percent higher and 7 percent lower than the initial stiffness values of Test A and Test B, respectively. All three tests showed comparable stiffnesses throughout testing.
2. The ultimate load of specimens tested with walls (Test C) was approximately 8 to 10 percent lower than those with steel beams (Tests A and B) and was

reached at a displacement of 38% and 29% lower than Tests A and B, respectively. This was due to the increased ductility of the system when using steel beams with shear studs.

3. The predominant failure mode was diagonal tension failure for all three tests and thus exhibited "low" strength capacities at high displacements due to the cracks penetrating through the plank depth.
4. The ultimate load of Test C was attained at approximately 50 percent higher displacement than Test A and B. Similar diaphragm behavior was observed when comparing the virgin and stabilized envelopes except a slight difference in behavior of the specimen with concrete masonry walls in the positive displacement region due to the unsymmetrical failure.
5. The initial edge zone force distribution, developed in References 20 and 50, was verified by finite element analysis for diaphragm with walls resulting in a slightly different edge zone distance due to flange action of the masonry walls.
6. The predictive method for initial stiffness and FME gave results in close agreement with experimental data.
7. The connection type and details exhibited good performance and withstood the induced forces in the system and caused the first failure to occur in the diaphragm.
8. Wall-to-wall connection contributed to increasing the edge zone distance due to increased flange width of wall.
9. The finite element analysis showed that about 30% of the load is transferred from loading wall to floor through the flange of wall region. It also showed that the initial stiffness of specimen is mostly controlled by the stiffness of the fixed support.
10. The slab dowel configuration within the topping enhanced the edge zone stiffness and prevented failure occurrence near the interface, forcing crack development outside the edge zone region.
11. Since the connection between the walls and the floor diaphragm did not crack, the interface is considered to be infinitely stiff.
12. The grout in cores of planks in the front edge added to the strength and stiffness of the connection and enabled it to transfer load to floor diaphragm more safely.
13. The grout in cores of planks in back (restrained) edge, with the reinforcement that is used for attachment caused excessive cracking development at end of grout.
14. The prestressing strands caused concrete spalling within the bottom wythe of the planks.
15. No separation between the topping and planks was observed indicating an ideal bond between the two.
16. The high tensile stresses due to cantilever action near the back edge of the specimen caused cracks at connection of side walls to back wall.
17. The inelastic behavior of the masonry walls after cracking caused a decrease in the peak strength of the diaphragm.

18. The test results have demonstrated that appropriate connections between reinforced concrete masonry walls and floor diaphragms, forming a box-type system, can exhibit a certain extent of strength capability under cyclic displacement reversals, and are, therefore, capable of attaining, rather exceeding, the strength of the topped hollow-core plank diaphragm.

6.3. Recommendations for Further Study

1. Perform additional diaphragm tests with various connection details and determine what effect the connection stiffness has on the diaphragm behavior.
2. Conduct tests with planks oriented in the direction parallel to the load direction so planks are adjacent to the loading wall, rather than supported by it, so side wall connection detail is used eliminating the contribution of grout in cores to the load transfer mechanism.
3. Determine the effect of fixing the bottom edge of walls and applying cyclic load at the top to include the effect of torsion of side walls on the connection, which more closely models the actual loading on connections in reality.
4. Determine the effects of superimposed vertical load on the overall behavior of diaphragm.
5. Complete a three-dimensional finite element analysis in order to determine the load path and transfer mechanism from walls to diaphragm through the connections.
6. Perform a sensitivity study to determine the effect of various assumptions utilized in determining the initial stiffness, FME and limit state strengths and to more accurately predict the behavior of such systems.
7. Determine the effects of out-of-plane forces and displacements on in-plane behavior of the shear transfer mechanism and boundary connections.
8. Investigate the effects of utilizing an interior wall as the loading wall.
9. Perform additional diaphragm tests on untopped planks with the appropriate connection details.
10. Perform more tests with various connection types and details so that the first failure occurs in the interaction region.
11. Prepare a set of design recommendations and a design procedure for hollow-core plank diaphragms and their connections to masonry walls.
12. Use some type of reinforcement within the bottom wythe of the planks to prevent excessive spalling of concrete during high displacement reversals.

7. ACKNOWLEDGEMENTS

This research was conducted at Iowa State University under the auspices of the Engineering Research Institute. The work was conducted in the Structural Engineering Laboratories in the Department of Civil and Construction Engineering. This investigation was sponsored by the National Science Foundation, Grant No. BCS-8722870. The work is part of the United States - Japan Coordinated Program for Masonry Building research conducted under the auspices of the Panel on Wind and Seismic Effects of the U.S.-Japan Natural Resources Development Program (UJNR).

The planks for the research were provided by Prestressed Concrete Operations, a division of Wheeler Consolidated. The materials for the walls were donated by the Masonry Institute of Iowa. The contribution of a graduate fellowship by the National Concrete Masonry Association is acknowledged.

The authors wish to thank all of the above sponsors of this work. In addition, the authors thank the TCCMAR Committee members and TCCMAR Chair, James Noland, for their input during the investigation. Acknowledgement is also due for the help of Mr. Douglas Wood, Laboratory Supervisor, Mr. Bruce Barnes, Assistant Scientist, and numerous hourly graduate and undergraduate students who assisted with the work.

8. REFERENCES

1. Anvar, A., S. K. Arya and G. A. Hegemier. "Behavior of Floor-to-Wall Connections in Concrete Masonry Buildings." In Proceedings of the Second North American Masonry Conference, edited by D. W. Vannoy and J. Colville, University of Maryland, College Park, Maryland, August 9-11, 1982.

2. Mayes, R. L. and R. W. Claugh. "A Literature Survey - Compressive, Tensile, Bond and Shear Strength of Masonry." Report No. EERC 75-15, University of California, Berkeley, California, 1975.

3. Hegemier, G. A. "Mechanics of Reinforced Concrete Masonry: A Literature Survey." Report No. AMES-NSF TR-75-5, University of California, San Diego, LaJolla, California, 1975.

4. Mayes, R. L. and R. W. Claugh. "State-of-the-Art in Seismic Shear Strength of Masonry - An Evaluation and Review." Report No. EERC 75-21, University of California, Berkeley, California, 1975.

5. Hegemier, G. A., S. K. Arya, R. O. Nunn, M. E. Miller, A. Anvar and G. Krishnamoorthy. "A Major Study of Concrete Masonry Under Seismic-Type Loading." Report No. UCSD/AMES/TR-77/002, University of California, San Diego, LaJolla, California, 1977.

6. Nunn, R. O. "Planar Mechanics of Fully Grouted Concrete Masonry." Ph.D. Dissertation, University of California, San Diego, LaJolla, California, 1980.

7. "Test Report on Slender Walls." ACI-SEASC Task Committee on Slender Walls, edited by J. W. Athey, Los Angeles, California, September, 1982.

8. Mackintosh, A. and W. L. Dickey. "Results of Variation of 'b' or Effective Width in Flexure in Concrete Block Panels." Masonry Industry of America, Los Angeles, California, 1971.

9. Roberts, J. "The Behavior of Vertically Reinforced Concrete Blockwork." Proceedings of the First Canadian Masonry Symposium, University of Calgary, Canada, June 7-10, 1976.

10. Gajer, R. B. "Minimum Steel Requirements for Masonry Walls, Out-of-Plane Forces." M.S. Thesis, Department of Civil Engineering, University of British Columbia, Vancouver, Canada, January, 1982.

11. Porter, M. L. and A. A. Sabri, "Plank Diaphragm Characteristics." U.S.-Japan Coordinated Program for Masonry Building Research, Final Report Task 5.1., Department of Civil and Construction Engineering, Iowa State University, Ames, Iowa, 1990.

12. Clough, D. P., "Considerations in the Design of Precast Concrete Diaphragms for Earthquake Loads.", Proc. of a Workshop on the Design of Prefabricated Concrete Buildings for Earthquake Loads., Applied Technology Council, Berkeley, California, 1981.

13. "Seismic Design for Buildings." Technical Manual TM 5-809-10, Departments of the Army, the Navy, and the Air Force, Washington D.C., February 1982.

14. Noland, J. L. "U.S. Research Plan.", U.S.-Japan Coordinated Program for Masonry Research, Typescript, Atkinson-Noland and Associates, Boulder, Colorado, 1984, Revised 1985.

15. Porter, M. L., F. S. Yeomans and A. W. Johnson, "Assembly of Existing Diaphragm Data." U.S.-Japan Coordinated Program for Masonry Building Research, Final Report Task 5.2., Department of Civil and Construction Engineering, Iowa State University, Ames, Iowa, 1990.

16. Gates, W. E. "Seismic Design Consideration for Untopped Precast Concrete Floor and Roof Diaphragms." Proceedings of a Workshop on the Design of Prefabricated Concrete Buildings for Earthquake Loads. Applied Technology Council. Berkeley, California, 1981.

17. Concrete Technology Associates. "Shear Diaphragm Capacity of Precast Floor Systems." Technical Bulletin 73-136, Concrete Technology Associates, Tacoma, Washington, June, 1973.

18. Martin, L. D. and W. J. Korkosz. "Connections for Prestressed Concrete Building Including Earthquake Resistance." Prestressed Concrete Institute, Chicago, Illinois, 1985.

19. Hawkins, N. M. "State-of-the-Art Report on Seismic Resistance of Prestressed and Precast Concrete Structures, Part I, II." Journal of Prestressed Concrete Institute, 22, No. 6 (Nov.-Dec. 1978), pp. 80-110.

20. Fuller, G. R. "Seismic Resistance vs. Progressive Collapse of Precast Concrete Panel Buildings." Proceedings, Workshop on Earthquake Resistant Reinforced Concrete Buildings Construction, University of California at Berkeley, July, 1977.

21. Engineering Testing Laboratories, Inc. "Reports on Horizontal Shear Tests of Span-Deck Grouted Edge Joints." Prepared by Tanner Prestressed and Architectural Concrete Co., Inc., Phoenix, Arizona, March, 1973.

22. Reinhardt, H. W. and H. W. Hartjes. "Invloed Van de Voeglente op de Afschufsterke Von Voegen Tussen Geprefabricereerde Kanaalplanten." Cement 34, No. 3, (1982): 185-187.

23. Sahlin, S. "Interaction of Brick Masonry Walls and Concrete Slabs." Designing, Engineering, and Construction with Masonry Products, Edited by F. B. Johnson, Gulf Publishing Company, Houston, Texas, 1969.

24. Harris, H. G. and I. J. Becica. "Behavior of Concrete Masonry Structures and Joint Details using Small Scale Direct Models." Paper No. 10, Proceedings of the North American Masonry Conference, edited by J. L. Noland and J. E. Amrhein, University of Colorado, Boulder, Colorado, August 14-16, 1978.

25. Gulkan, P., R. L. Mayes and R. W. Clough. "Strength of Timber Roof Connections Subjected to Seismic Loads." Report No. UCB/EFRC-78/17, University of California, Berkeley, California, 1978.

26. Paulay, T., R. Park and M. H. Phillips. "Horizontal Construction Joints in Cast-in-Place Reinforced Concrete." Shear in Reinforced Concrete, Publication SP-42, ACI, Detroit, Michigan, 1974.

27. Hofbeck, J. A., I. O. Ibrahim and A. H. Mattock. "Shear Transfer in Reinforced Concrete." Proceedings ACI Journal, Vol. 66, No. 2, February, 1969, pp. 119-128.

28. Leombruni, P., O. Buyukozkurk and J. J. Conner. "Analysis of Shear Transfer in Reinforced Concrete with Application to Containment Wall Specimens." Report No. NUREG/CR-1085RD, Massachusetts Institute of Technology, Cambridge, Massachusetts, 1979.

29. Jimenez-Perez, R., P. Gergely and R. N. White. "Shear Transfer Across Cracks in Reinforced Concrete." Report No. 78-4, Cornell University, Ithaca, New York, 1978.

30. Laible, J. P., R. N. White and P. Gergely. "Experimental Investigation of Seismic Shear Transfer Across Cracks in Concrete Nuclear Containment Vessels." Reinforced Concrete Structures in Seismic Zones, Publication SP-53, ACI, Detroit, Michigan, 1977.

31. Birkeland, D. W. and H. W. Birkeland. "Connections in Precast Concrete Construction." Proceedings, ACI Journal, Vol. 63, No. 3, March, 1966, pp. 345-368.

32. Mast, R. F. "Auxiliary Reinforcement in Concrete Connections." Proceedings, ASCE, Vol. 94, ST6, June, 1968, pp. 1485-1504.

33. Loeber, P. J. and Paulay, T. "Shear Transfer by Aggregate Interlock." Shear in Reinforced Concrete, Publication SP-42, ACI, Detroit, Michigan, 1974.

34. Dulaeska, H. "Dowel Action of Reinforcement Crossing Cracks in Concrete." Proceedings, ACI Journal, Vol. 69, No. 12, December, 1972, pp. 754-757.

35. Jimenez, R., R. N. White and P. Gergely. "Cyclic Shear and Dowel Action Models in Reinforced Concrete." Proceedings, ASCE, Vol. 108, No. ST5, May, 1982, pp. 1106-1123.

36. American Society for Testing and Materials, 1986 Annual Standards, Section 4, Vol. 04.05, 1986.

37. Uniform Building Code Standards, 1988 Edition, The International Conference of Building Officials, Whitter, California, 1988.

38. Porter, M. L. and P. M. Tremel. "Sequential Phase Displacement." U.S. Japan Coordinated Program for Masonry Building Research, Task 5.1. Typescript, Iowa State University, Ames, Iowa, 1987.